

This Page Is Inserted by IFW Operations  
and is not a part of the Official Record

## **BEST AVAILABLE IMAGES**

Defective images within this document are accurate representations of the original documents submitted by the applicant.

Defects in the images may include (but are not limited to):

- BLACK BORDERS
- TEXT CUT OFF AT TOP, BOTTOM OR SIDES
- FADED TEXT
- ILLEGIBLE TEXT
- SKEWED/SLANTED IMAGES
- COLORED PHOTOS
- BLACK OR VERY BLACK AND WHITE DARK PHOTOS
- GRAY SCALE DOCUMENTS

**IMAGES ARE BEST AVAILABLE COPY.**

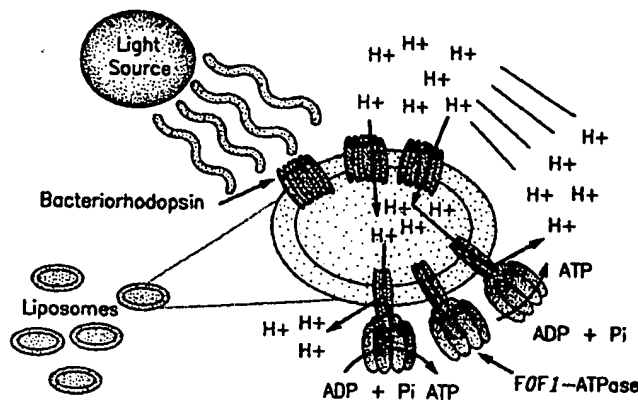
**As rescanning documents *will not* correct images,  
please do not report the images to the  
Image Problem Mailbox.**



## INTERNATIONAL APPLICATION PUBLISHED UNDER THE PATENT COOPERATION TREATY (PCT)

(51) International Patent Classification <sup>7</sup> : <b>C12N 9/14, 11/00, C07K 14/00, B82B 1/00, H02N 6/00, 11/00</b>		A2	(11) International Publication Number: <b>WO 00/22101</b>	
			(43) International Publication Date: 20 April 2000 (20.04.00)	
(21) International Application Number: <b>PCT/US99/23636</b>		(81) Designated States: AE, AL, AM, AT, AU, AZ, BA, BB, BG, BR, BY, CA, CH, CN, CU, CZ, DE, DK, EE, ES, FI, GB, GD, GE, GH, GM, HR, HU, ID, IL, IN, IS, JP, KE, KG, KP, KR, KZ, LC, LK, LR, LS, LT, LU, LV, MD, MG, MK, MN, MW, MX, NO, NZ, PL, PT, RO, RU, SD, SE, SG, SI, SK, SL, TJ, TM, TR, TT, UA, UG, <u>US</u> , UZ, VN, YU, ZA, ZW, ARIPO patent (GH, GM, KE, LS, MW, SD, SL, SZ, TZ, UG, ZW), Eurasian patent (AM, AZ, BY, KG, KZ, MD, RU, TJ, TM), European patent (AT, BE, CH, CY, DE, DK, ES, FI, FR, GB, GR, IE, IT, LU, MC, NL, PT, SE), OAPI patent (BF, BJ, CF, CG, CI, CM, GA, GN, GW, ML, MR, NE, SN, TD, TG).		
(22) International Filing Date: 13 October 1999 (13.10.99)		<p><b>Published</b> Without international search report and to be republished upon receipt of that report.</p>		
(30) Priority Data:				
60/104,062	13 October 1998 (13.10.98)			US
60/126,586	26 March 1999 (26.03.99)			US
60/152,983	9 September 1999 (09.09.99)	US		
(71) Applicant (for all designated States except US): CORNELL RESEARCH FOUNDATION, INC. [US/US]; Suite 105, 20 Thornwood Drive, Ithaca, NY 14850 (US).				
(72) Inventor; and				
(75) Inventor/Applicant (for US only): MONTEMAGNO, Carlo, D. [US/US]; 49 Besemer Hill Road, Ithaca, NY 14850 (US).				
(74) Agent: MICHAELS, Christopher, A.; Brown, Pinnisi & Michaels, P.C., Suite 400, 118 North Tioga Street, Ithaca, NY 14850 (US).				

(54) Title: ENZYMES AS A POWER SOURCE FOR NANOFABRICATED DEVICES



## (57) Abstract

A nanoscale engineered system includes the integration of at least one  $F_1$ -ATPase molecular motor with a nano-electro-mechanical system (NEMS). The resultant functional hybrid organic/inorganic nanomechanical system provides the ability to move nanotechnology into medical and physiologic applications. The ability to accurately and precisely position and orient individual proteins on a substrate is presented. Motive power for the nanomechanical systems disclosed is provided through the genetic expression and integration of at least one  $F_1$ -ATPase molecular motor, which utilizes ATP as a chemical energy source. In addition, the device is capable of being fuelled with light energy. The NEMS device can be controlled by an "on/off" switch genetically engineered into the  $F_1$ -ATPase. The NEMS consists of one or more silicon based mechanical devices capable of operating in liquid environments and performing a variety of functions. The  $F_1$ -ATPase motors are used to pump fluids and open and close valves in microfluidic devices, as well as provide mechanical drives and motive power for nanomechanical devices.

**FOR THE PURPOSES OF INFORMATION ONLY**

Codes used to identify States party to the PCT on the front pages of pamphlets publishing international applications under the PCT.

AL	Albania	ES	Spain	LS	Lesotho	SI	Slovenia
AM	Armenia	FI	Finland	LT	Lithuania	SK	Slovakia
AT	Austria	FR	France	LU	Luxembourg	SN	Senegal
AU	Australia	GA	Gabon	LV	Latvia	SZ	Swaziland
AZ	Azerbaijan	GB	United Kingdom	MC	Monaco	TD	Chad
BA	Bosnia and Herzegovina	GE	Georgia	MD	Republic of Moldova	TG	Togo
BB	Barbados	GH	Ghana	MG	Madagascar	TJ	Tajikistan
BE	Belgium	GN	Guinea	MK	The former Yugoslav Republic of Macedonia	TM	Turkmenistan
BF	Burkina Faso	GR	Greece			TR	Turkey
BG	Bulgaria	HU	Hungary	ML	Mali	TT	Trinidad and Tobago
BJ	Benin	IE	Ireland	MN	Mongolia	UA	Ukraine
BR	Brazil	IL	Israel	MR	Mauritania	UG	Uganda
BY	Belarus	IS	Iceland	MW	Malawi	US	United States of America
CA	Canada	IT	Italy	MX	Mexico	UZ	Uzbekistan
CF	Central African Republic	JP	Japan	NE	Niger	VN	Viet Nam
CG	Congo	KE	Kenya	NL	Netherlands	YU	Yugoslavia
CH	Switzerland	KG	Kyrgyzstan	NO	Norway	ZW	Zimbabwe
CI	Côte d'Ivoire	KP	Democratic People's Republic of Korea	NZ	New Zealand		
CM	Cameroon	KR	Republic of Korea	PL	Poland		
CN	China	KZ	Kazakhstan	PT	Portugal		
CU	Cuba	LC	Saint Lucia	RO	Romania		
CZ	Czech Republic	LI	Liechtenstein	RU	Russian Federation		
DE	Germany	LK	Sri Lanka	SD	Sudan		
DK	Denmark	LR	Liberia	SE	Sweden		
EE	Estonia			SG	Singapore		

## ENZYMES AS A POWER SOURCE FOR NANOFABRICATED DEVICES

### REFERENCE TO PROVISIONAL APPLICATION

This application claims an invention which was disclosed in Provisional Application Number 60/104,062, filed October 13, 1998, entitled "ENZYMES AS A POWER SOURCE FOR NANOFABRICATED DEVICES", Provisional Application Number 60/126,568, filed March 26, 1999, entitled "ENZYMES AS A POWER SOURCE FOR NANOFABRICATED DEVICES", and Provisional Application Number 60/152,983, filed September 9, 1999, entitled "ENZYMES AS A POWER SOURCE FOR NANOFABRICATED DEVICES". The benefit under 35 USC §119(e) of the United States provisional application is hereby claimed, and the aforementioned applications are hereby incorporated herein by reference.

### FIELD OF THE INVENTION

The invention pertains to the field of nanotechnology. More particularly, the invention pertains to the union of organic molecular motors with micromechanical devices to provide motive power for the hybrid devices in various liquid environments.

### BACKGROUND OF THE INVENTION

#### Nanotechnology

Nanotechnology is the miniaturization of mechanical devices to smaller and smaller dimensions, and provides the ability to mechanically manipulate molecules and molecular structures as an assembly and manufacturing process.

Nanofabrication entails the use of micro-machined components. Components that feature sizes as small as 0.1 microns are now within the realm of manufacturing feasibility. The capability to manufacture components this small has come as a result of rapid technological improvement in engineering expertise in the manufacture of integrated circuits for the computer industry. The microlithography techniques useful in the computer industry for etching transistor and conductor sites on standard silicon

wafers are now directly applied to creating ever-smaller micromachine components for a variety of industrial and commercial applications.

Currently, there is a significant drive to miniaturize mechanical devices for use as new types of sensors and actuators. These devices are usually made of silicon and other materials compatible with integrated circuit electronics. The source of power and control of these devices is in all cases electrical. The most common method of imparting motive forces to the moving mechanical devices is with the use of electric fields. The electric field approach works well for applications that involve a partial or near vacuum and in non-conducting gases, however, this is not compatible with conducting liquids such as saline solutions. This has been a severe limitation in the utilization of miniaturized mechanical devices in physiologically or medically relevant environments.

The present generation of Micro-Electro-Mechanical (MEMS) devices are generally made by photolithographic and chemical etching processes and are many micrometers in size. These are useful as accelerometers, flow meters, force transducers and a growing number of other applications. All such systems require electrical connections to the macroscopic world for power and control signals. The need to power microscale devices with macroscopic power sources has placed severe restrictions on the application of this technology to implants in living systems, as well as to the types of devices that can be devised for such use. Ideally, one would wish to obtain power for nanoscale implants directly from a biological system within which the nanotech device is implanted.

Efforts to power implants using the *in situ* power of the patient are not without precedent. Muscle stimulation devices with battery power supplies have helped a wide variety of patients for many years. This type of implant has been used successfully for dynamic cardio-myoplasty and electrostimulated graciloplasty for fecal incontinence (Lanmuller *et al.*, 1997). Unfortunately, there are many limitations associated with these battery-powered devices. Patients with these implants must still be subjected to follow up surgeries in order to replace a battery that fails (Medina and Michelson, 1985). There are also many patients that can not be treated with the battery-powered muscle stimulation devices. For example, no fully implantable device exists for the restoration of hand, leg, and breathing functions after paralysis due to spinal cord injury

(Lanmuller *et al.*, 1997). Cochlear implants cannot operate on a battery power supply because of issues associated with the signal processing required to translate sound into understandable information (Lanmuller *et al.*, 1997).

Integration of the nanoscale bio-compatible lithographic processes with biological molecular motors may provide the means for creating a transparent interface between the organic/inorganic world, preferably one that uses an organic power source.

### SUMMARY OF THE INVENTION

Briefly stated, the present invention of a nanoscale engineered system includes the integration of a molecular motor with a nano-electro-mechanical system (NEMS). The nanofabricated device specifically utilizes at least one chemical enzyme that undergoes a conformational shift. For example,  $F_1$ -ATPase is the molecular motor.  $F_1$ -ATPase is a ubiquitous enzyme capable of creating energy by using ATP as a chemical energy source. The functional hybrid organic/inorganic nanomechanical system resulting from the union of nanotechnology and biochemistry provides the ability to move the field into medical and physiologic applications. The ability to accurately and precisely position and orient individual proteins on a substrate is presented. Motive power for the nanomechanical systems incorporated into hybrid devices is provided through the genetic expression and integration of at least one  $F_1$ -ATPase molecular motor, which utilizes ATP as a chemical energy source. An integrated  $F_1$ -ATPase powered NEMS device that is fueled by light-driven ATP production is demonstrated. The recombinant  $F_1$ -ATPase motor protein can also be genetically modified so that it can be controlled by a secondary chemical system, thereby creating an effective on/off switch for the device. The NEMS consists of one or more silicon based mechanical devices capable of operating in liquid environments and performing a variety of functions. The  $F_1$ -ATPase motors are used to pump fluids and open and close valves in microfluidic devices, as well as provide mechanical drives and motive power for nanomechanical devices.

In an embodiment of the present invention, a method of attaching a protein to a substrate is presented. A molecular support on a protein is bound to a pattern of molecules found in a site specific location on the substrate. By utilizing two or more

site specific locations on the substrate in sufficient proximity to each other, two or more proteins can operatively associate to perform sequential enzymatic reactions.

Another embodiment of the present invention includes a substrate with a pattern of molecules etched onto a site specific location on the substrate. The pattern of molecules is capable of binding to a molecular support genetically engineered into a protein. More complex structures including two or more site specific locations on the substrate in sufficient proximity to each other allow two or more proteins to operatively associate to perform sequential enzymatic reactions.

In another embodiment of the present invention, a nanoscale-engineered system includes at least one Nano-Electro-Mechanical System (NEMS) operatively connected to and harnessing mechanical motion of a portion of at least one ATP synthase complex.

In another embodiment of the present invention, an expression vector includes a portion of an ATP synthase complex expressed in an expression vector. The expression of the portion of the ATP synthase complex allows for its attachment to a nano-electro-mechanical system.

Another embodiment of the present invention is a method of providing motive force to a nanoscale engineered system. ATP molecules are generated with the ATP synthase complex, and an F1 subunit of the ATP synthase complex is used to generate energy for the nanoscale engineered system.

Another embodiment of the present invention includes an integrated F<sub>1</sub>-ATPase powered NEMS device fueled by light-driven ATP production. This device is capable of generating energy with ATP.

Another embodiment of the present invention includes control of the NEMS device by a genetically engineered component such as a secondary chemical signal. This embodiment essentially creates an "on/off" switch capable of controlling the activity of the F<sub>1</sub>-ATPase motor.

In another embodiment of the present invention, a method of detecting the molecular rotation of a molecular motor includes attaching a molecular tag that is readily visible under an optical microscope to a structural element of the molecular motor being to be observed and then monitoring or recording the movement of the molecular motor.

### BRIEF DESCRIPTION OF THE DRAWINGS

FIG. 1 shows the structure of ATP synthase molecule, with the  $F_0$  portion located in the membrane and the  $F_1$  portion, which is responsible for ATP hydrolysis.

FIG. 2 shows the ratchet type motion of the  $F_1$ -ATPase molecular motor.

FIG. 3 shows the configuration of the  $F_1$ -ATPase motor-actin filament system.

FIG. 4 shows the assembly of the  $F_1$ -ATPase – microsphere system.

FIG. 5 shows the attachment of His-tagged 1  $\mu$ m microspheres to gold, copper, and nickel coated coverslips.

FIG. 6 shows ATP production in engineered liposomes containing bacteriorhodopsin and  $F_0F_1$ -ATPase.

FIG. 7 shows the number of liposomes, at various rates of ATP production, required to continuously power a single  $F_1$ -ATPase motor at different rotational velocities: 1 ( $\blacklozenge$ ), 5 (+), 10 ( $\blacktriangle$ ), 15 ( $\bigcirc$ ), and 17 ( ) r.p.s.

FIG. 8 shows the length of one side of a light harvesting device, at various rates of ATP production, required to continuously power a single  $F_1$ -ATPase motor at different rotational velocities: 1 ( $\blacklozenge$ ), 5 (+), 10 ( $\blacktriangle$ ), 15 ( $\bigcirc$ ), and 17 ( ) r.p.s.

FIG. 9 shows an idealized construction of a photonic,  $F_1$ -ATPase powered NEMS device.

FIG. 10 shows the chemical control of a  $F_1$ -ATPase powered intracellular nanomechanical device.

FIG. 11 shows the chemical control of  $F_1$ -ATPase using a unique zinc binding site engineered into the  $\alpha$  and  $\beta$  subunits. Initially, zinc will bind to a unique site an inactive the motor. The addition of EDTA will chelate the zinc ions, and re-activate the motor allowing rotation of the  $\gamma$  subunit.

### DESCRIPTION OF THE PREFERRED EMBODIMENT

Referring to FIG. 1, nanoscale engineered systems are composed of silicon-based nanomechanical components joined with a variety of biological molecules including molecular motors. In this way hybrid nanoscale engineered systems that harness the mechanical motion of the biological motor protein  $F_1$ -ATPase as a source of motive power can be combined with the precision of micromachined integrated circuits to perform a wide variety of functions in liquid environments. The ability to accurately and precisely position and orient individual motors on a surface is provided. To further harness the energy of this system, an efficient way to fuel the device is presented, as well as an "on/off" switch capable of controlling the output of the device.  $F_1$ -ATPase motors can be used in conjunction with silicon-based components to pump fluids and open and close valves in microfluidic devices, and provide mechanical drives for a new class of nanomechanical devices. The elimination of electrical wires and electrostatic drives that do not operate in water will remove significant limitations inherent in the silicon mechanical systems of the past.

Recent research has explored the use of advanced nanofabrication processes to create mechanical devices with dimensions of tens of nanometers. By the use of electron beam lithography, mechanical springs and moving objects can be fabricated in a wide range of geometries with spring constants below a Newton/meter. Optical techniques can be used to observe nanometer scale motion by interference. We thus have the capability to create and observe the motion of inorganic mechanical devices on a scale compatible with the molecular motors. This ability to observe nanoscale components and molecular motors also allows the ability to monitor and test any hybrid device that is the union of these underlying components.

The processes for coupling organic systems to silicon and other inorganic surfaces involves the use of patterned monolayers and genetically modified proteins. The use of electron beam lithography again provides a method of modifying surface chemical properties on a nanometer scale. This approach will provide the mechanism for appropriately uniting the organic and inorganic components of the hybrid systems. The necessary biological system for producing genetically engineered variants of the  $F_1$ -ATPase biomolecular motor has been established.

Because the  $F_1$ -ATPase biomolecular motor is produced by cellular physiology and the scale of a Nano Electro Machine System (NEMS) is considerably smaller than that of a single cell, it is possible to insert the NEMS into a cell where the motor and NEMS could be self-assembled by the host cell's physiology. Given that the motor itself is part of the ATP synthase complex, the motor performs its function through the application of chemical energy in the form of adenosine triphosphate (ATP). The host cell's physiology possibly can also be utilized to replace molecular motors when they cease to function.

Through the precise manipulation of molecular motors and nano scale machine components, a fully implantable bioNEMS system that incorporates real-time blood gas and chemical analysis to control and regulate breathing of paralyzed patients can be realized. It should also be possible to develop an implant that automatically monitors the physiology of the patient to administer pharmacokinetic agents. Recently investigators at the Cornell University Nanofabrication Facility have made an artificial cochlea using MEMS technology (McDonald, 1996). A more advanced biomolecular motor powered version of this device could be an effective prosthetic.

#### Energy in the Biological World

An important feature of living systems is the ability to transform a diverse array of highly specific sources of energy into a generic energy currency that can be universally used by cells or enzymes. This energy currency, Adenosine triphosphate or ATP, is the energy source used by virtually every living organism.

### Molecular Motors

Cells employ a variety of linear motors, including myosin, kinesin and RNA polymerases, which move along and exert force on a filamentous structure. In biology this type of motor is most often associated with the flagellum of bacteria or sperm. An alternative motor structure is the rotary motor. The only known example of the molecular rotary motor is the ATP synthase enzymatic complex that reversibly couples the transmembrane flow of protons to ATP synthesis/hydrolysis in respiring cells and photosynthetic cells.

ATP synthase is an ubiquitous enzyme that is found in aerobic, anaerobic and photosynthetic bacterial membranes, the mitochondria of animal cells and in the chloroplasts of plant cells. The function of ATP synthase is to synthesize or hydrolyze ATP by utilizing the proton electrochemical gradient across energy transducing membranes.

ATP synthase is composed of two separate parts, F<sub>0</sub>, a hydrophobic part that is located in the membrane and is responsible for mediating protein translocation, and F<sub>1</sub>, the hydrophilic portion of the molecule which is located next to the membrane and contains the sites to catalyze the hydrolysis of ATP. It is believed that the energy exchange between the F<sub>1</sub> and F<sub>0</sub> ATPases is regulated by the 7 subunits of the F<sub>1</sub>-ATPase complex (Yasuda *et al.*, 1997).

Based upon the structure of the F<sub>1</sub>-ATPase, the mechanism for controlling the flow of the energy between the two parts of ATP synthase is the rotary motion of the  $\gamma$  subunit relative to the  $\alpha_3\beta_3$  subassembly. This model suggests a ratchet type motion for the  $\gamma$  subunit. The  $\gamma$  subunit moves in discrete steps between the catalytic nucleotide binding sites of the  $\alpha\beta$  complexes. The interaction between the  $\gamma$  subunit and the  $\alpha\beta$  complexes causes a distortion of the F<sub>0</sub> subunits thereby modulating the catalytic properties of the nucleotide binding sites and thus facilitating the synthesis/hydrolysis of ATP.

Referring to FIG. 2, the F<sub>1</sub>-ATPase portion has a central rotor of radius approximately 1 nm, formed by its gamma-subunit, which turns in a stator barrel of radius approximately 5nm formed by three  $\alpha$  and three  $\beta$  subunits. The  $\gamma$ -subunit of the F<sub>1</sub>-ATPase rotates within the  $\alpha\beta$ -hexamer. This conclusion is supported by studies

in which a fluorescent actin filament was attached to the  $\gamma$ -subunit as a tag. In the presence of ATP, the filament rotated for more than 100 revolutions in an anticlockwise direction when viewed from the 'membrane' side. The rotary torque produced by the observed rotation reached more than 40 pN nm(-1) under high load.

A rigorous evaluation of the engineering properties of the  $F_1$ -ATPase motor protein necessitates the development of assays that provide consistent measurements of the performance of the  $F_1$ -ATPase motor protein under different operating conditions. By integrating the  $F_1$ -ATPase motor protein with NEMS specifically designed to evaluate motor performance, the basic mechanics of motor protein motion and a technological foundation for functionally integrating these molecules with manufactured devices can be devised.

Referring to FIG.3, in March, 1997 Noji *et al.* demonstrated conclusively that the  $\gamma$  subunit of the membrane protein  $F_1$ -ATPase rotated in response to the synthesis/hydrolysis of ATP. The force generated by this motor protein (>100 pN) is among the greatest of any known molecular motor. The  $F_1$ -ATPase protein has a calculated no-load rotational velocity of 17 r.p.s. and a diameter of less than 12 nm. These properties coupled with the fact that  $F_1$ -ATPase is automatically synthesized as a normal part of cellular replication and ongoing protein production opens the door to potential of creating chemically powered nanomechanical devices. Using known genetic engineering techniques it is possible to isolate the genes coding for the ATP synthase complex, sequence them and then insert them into a desirable genetic expression vector such that desirable quantities of a modified  $F_1$ -ATPase molecular motor can be produced. Thereafter integration of the  $F_1$ -ATPase molecule with silicon-based Nano-Electro-Mechanical Systems (NEMS) can be done by uniting the modified handles of the  $F_1$ -ATPase structure with the hands of a prospective NEMS.

To enhance efficiency and effectiveness any nanoscale engineered system that is designed to function inside a living organism or biological system should be powered by ATP or other available chemical energy storage biomolecule. The use of ATP or other energy storage biomolecule by nanomachines or hybrid nanomechanical systems allows the creation of hybrid devices that integrate with biological systems at the most fundamental level. Through the integration of the  $F_1$ -ATPase molecule into a NEMS, the resultant hybrid nanoscale engineered system no longer requires attachment or

energy input from the macroscopic world and could operate independently for an indefinite time period.

### Rotary Motor Activity

Symbiosis among micro machine components, nano structure integration elements, and the protein products of genetic engineering techniques allows the development of micro and nano cybernetic enhancements to human scientific endeavor, human health, and lifestyle.

Referring also to FIG. 1, the  $F_1$ -ATPase expressing genes of the thermophilic bacterium *Bacillus PS3* are extensively modified and overexpressed in *E. coli*. The modified enzymatic product retains its action as a molecular motor though it contains only the aft subunits of the  $F_1$ -ATPase subassembly, because the  $\epsilon$  and  $\delta$  subunits are not necessary for the hydrolysis of ATP. The modifications to the  $F_1$ -ATPase expressing genes include attaching a 10 Hist-reporter tag to the N terminus of each subunit and biotinylating a cysteine that replaced the Ser107 residue in subunit 7t.

More specifically, the  $F_1$ -ATPase coding sequence ( $\alpha$ ,  $\beta$ , and  $\gamma$  subunits) is isolated from *Bacillus PS3* (Matsui and Yoshida 1995) using the polymerase chain reaction (PCR). Restriction endonucleases sites, *Bam*HI and *Pst*I, are added to the 5' and 3' end of the coding sequence, respectively, and used to directionally clone the 3.9 kb PCR product into the plasmid pGEM-3Z f(-). Subsequently, site directed mutagenesis is used to: (1) change the  $\alpha$ Cys193 to Ser, (2) change the  $\gamma$ Ser107 to Cys, (3) change the  $\gamma$  initiation codon from GTG to ATG, and (4) change the  $\gamma$  termination codon from TAG to TAA. In addition, a ten histidine (His) tag is inserted immediately downstream of the  $\beta$  initiation codon.

The mutated construct, pGEM-AITG, is then cloned into the expression plasmid pQE-30, which adds a six His tag to the N-terminus of the  $\alpha$  subunit. The expression plasmid pQE-MH is inserted into *Escherichia coli* JM103  $\Delta(uncB-uncD)$  in which the majority of  $F_1$ -ATPase genes have been eliminated; thus, minimizing/eliminating the formation of chimeric  $F_1$ -ATPases. Previous research demonstrated a 40% reduction in enzymatic activity associated with the addition of His tags to the  $F_1$ -ATPase from *E.*

*coli* (Ekuni *et al.*, 1998). For this reason, the mutated  $F_1$ -ATPase construct without His tags on the  $\beta$  subunit also is cloned into pQE-30, and expressed in *E. coli* JM103.

Further, the His tags on the  $\alpha$  subunit can be removed from the recombinant  $F_1$ -ATPase using thrombin, which cleaves directly downstream of the His tags. This expression system (pQE-M) is used to evaluate the effect of the His tags on both the  $\alpha$  and  $\beta$  subunits on motor performance. Together, pQE-M and pQE-MH provide flexibility in assessing motor performance and the effects of adding attachment handles to particular regions of the enzyme.

Expression of the recombinant  $F_1$ -ATPase is induced by the addition of 1 mM IPTG approximately 3 hours after inoculation of M9 minimal media. Native protein is extracted using lysozyme/sonication, and purified using  $Ni^{2+}$ -NTA affinity chromatography. Approximately 50 mg of  $F_1$ -ATPase is purified per liter of cell extract, and analyzed using SDS-polyacrylamide gel electrophoresis. The activity of the purified protein is measured using an ATP regeneration assay being known in the art, and incorporated by reference (Matsui and Yoshida, 1995; Matsui *et al.*, 1997).

The modified  $F_1$ -ATPase is then bound to a glass plate that is coated with horseradish peroxidase conjugated with  $Ni^{2+}$ -nitrilotriacetic acid (Ni-NTA). This compound has a strong affinity for a Histidine-tag. After washing, the  $F_1$ -ATPase complex is attached to the glass coverslip with the  $F_0$  portion of the ATP synthase molecule being separated from the glass surface. A fluorescently labeled biotinylated actin filament is then attached to the  $\gamma$  subunit of the  $F_1$ -ATPase complex. They are attached using streptavidin.

The activity of the  $F_1$ -ATPase-actin filament system is illustrated in FIG. 3. A single molecule of  $F_1$ -ATPase is by itself a rotary motor in which a central gamma subunit rotates against a surrounding cylinder made of the  $\alpha, \beta$  subassembly. Driven by three catalytic betas, each fueled with ATP, the central gamma subunit makes discrete 120-degree steps, occasionally reversing itself. The work done in each step is constant over a broad range of imposed loads and is close to the free energy of hydrolysis of one ATP molecule.

Analysis of the results of this experiment indicate that the force generated by this motor is a function of load and that the  $F_1$ -ATPase motor protein has the potential

of generating forces  $>100$  pN. The forces and loads were calculated using the data presented by Noji *et al.* (1997) and analyzed using the methods described by Hunt *et al.* (1994). Noji's analysis underestimates the force generated by the  $F_1$ -ATPase motor protein because it fails to account for the increase in viscous drag due the close proximity of the actin filament to the glass surface ( $\sim 5$  nm). Estimates are that Noji's analysis may underestimate the force generated by as much as a factor of 3 (Hunt *et al.*, 1994).

The power generated by the  $F_1$ -ATPase motor protein is relatively constant. Based upon bulk hydrolysis experiments, the no-load rotational velocity of the  $F_1$ -ATPase motor protein should be of the order of 17 r.p.s or approximately 1000 r.p.m. What was observed in Noji *et al.*'s experiment was that rotational velocity of the  $F_1$ -ATPase motor protein varied as a function of actin filament length. The longer the filament, the greater the load, and the slower the motor turned. The  $F_1$ -ATPase motor is capable of producing an astounding amount of power for its size. The actin filaments used in this experiment varied in size from 1 to 3  $\mu$ m. The diameter of the rotor is approximately 1 nm, while the diameter of the entire motor is only about 10 nm. The average angular velocity of the  $F_1$ -ATPase motor protein when it was attached to the 2  $\mu$ m actin filaments was almost 1 r.p.s. The performance of this motor is equivalent to a man spinning a 2000 ft long stick, 6 ft in diameter, in the water, at 60 r.p.m. The performance of this molecule establishes the possibility of incorporating a biomotor powered NEMS into a cellular system that uses the machinery of the cell to assemble, maintain and fuel an engineered device.

The force generated by the  $F_1$ -ATPase motor protein ( $>100$  pN) is among the greatest of any known molecular motor (Noji *et al.*, 1996). With a calculated no-load rotational velocity of 17 r.p.s. and a diameter of less than 12 nm the  $F_1$ -ATPase protein is a tailor made nano-motor. These properties, coupled with the fact that  $F_1$ -ATPase is automatically synthesized using the machinery of life, open the door to the potential of creating hybrid organic/inorganic NEM devices. The  $F_1$ -ATPase motor protein has the potential to become a cornerstone in the seamless integration of nano-devices with living systems.

The observed rotational speed of the  $F_1$ -ATPase motor is, in fact, quite high when taking into account the hydrodynamic friction acting against the rotating actin

filament. If the internal 1 nm filament were scaled to the size of a person, the person would be standing at the bottom of a large swimming pool rotating a 500 m rod at several revolutions per second. The torque the molecular  $F_1$ -ATPase, produced to overcome the friction amounted to approximately 40 pN - nm over a broad range of rotational speed (Noji *et al.*, 1997). Roughly speaking, the mechanical work done in one third of a revolution is 80 pN - nm. This work is comparable to the free energy of hydrolysis of one ATP molecule, also at approximately 80 pN - nm. If one ATP is consumed per 120-degree rotation, the efficiency of our  $F_1$ -ATPase motor is nearly 100%.

#### Union of Biotechnology and Nanotechnology

Molecular biology, like molecular nanotechnology, embraces the study of molecular machines and molecular machine systems. Ribosomes, like mechanisms in flexible molecular manufacturing systems, can be viewed as numerically controlled machine tools following a series of instructions to produce a complex product. Molecular biology and biochemistry stimulated the train of thought that led to the concept of molecular manufacturing, and their techniques offer paths to the development of molecular manufacturing systems.

Two scientific obstacles had to be overcome before it was possible to consider powering engineered silicon devices with motor proteins. First a system for modifying and producing  $F_1$ -ATPase motor protein in a form suitable for harnessing the power generated by this enzyme had to be developed. A system has been successfully developed to express the thermophilic *Bacillus PS3 F1*-ATPase protein in *E. coli*. This protein expression system provides a flexible platform from which we can place different "chemical" handles on the protein, thus establishing a means to integrate the molecular motor with NEMS.

The second challenge is the development of a methodology to precisely position and orient proteins onto a substrate. The development of electron beam lithography with organic monolayers (Lercel *et al.*, 1996, Carr and Craighead, 1997) provides this technology. This surface chemistry modification process is compatible with both biological molecules and semiconductor manufacturing processes (St John, *et al.*, 1997). It facilitates the placement of either single groups or designed patterns of

molecules with a precision of within 10 nm. This technology is used to place "hands", or patterns of molecules, at site specific locations on the substrate, for example an NEMS, that then grab the "handles", or molecular supports, genetically engineered into the protein, for example an  $F_1$ -ATPase motor, generated by a desirable genetic expression vector. This direct interface provides for a complementary binding system of "hands" and "handles" that permits the transfer of mechanical energy from the  $F_1$ -ATPase motor protein to the NEMS. An array of a pattern of molecules attached to site specific locations on the substrate is also possible using this technology. Utilizing two or more site specific locations in sufficient proximity to each other on the substrate allows for two or more proteins to operatively associate to perform sequential enzymatic reactions.

To integrate biomolecular motors into NEMS, procedures for the specific attachment, positioning, and orientation of these motors is essential. Therefore, an evaluation of the binding of biological molecules to nanofabricated substrates is necessitated. Electron beam lithography is utilized to etch an array pattern on a 25 mm coverslip that had been coated with a resist bilayer. As an example, the coverslips are patterned with metal substrates using evaporative deposition of gold, copper, or nickel. Other materials, including other metals such as iron, and polymers, which have an affinity for an enzymatic tag, can also be applied as substrates. Subsequently, the bilayer is removed to expose the array.

Evaporative deposition is used to coat glass coverslips (24 x 60 mm, 0.13 – 0.17 mm in thickness; Clay Adams Inc.) with 200 Å of gold (Au), copper (Cu), or nickel (Ni) for the bonding substrates. Blank glass coverslips coated with the microsphere solution are used to establish a baseline for comparison of bonding strengths among the various metallic surfaces. Several glass coverslips coated with 500- $\mu$ l of 1% nitrocellulose in amyl acetate (Sigma Chemical Co., St. Louis, MO) are used to establish a baseline for comparing the bonding strengths among the metallic substrates.

Coverslips are thoroughly cleaned before utilization in flow tests or in substrate preparation to ensure oil, dirt, and other residues are properly removed and do not affect adhesion strength evaluations. Coverslips are immersed for at least twenty-four hours in a solution of 36N  $H_2SO_4$  and NoChromix® followed by rinsing with deionized water.

Subsequently, the rinsed coverslips are incubated in boiling water for approximately 15 minutes and air-dried. Cleaned coverslips are handled using forceps to minimize contact with surfaces.

Thin metallic film deposition is performed using thermal evaporation in a vacuum chamber and a pressure of approximately  $10^{-5}$  torr. Chrome is first heated to 1900 Kelvin (to achieve 1 Torr vapor pressure), and then applied on coverslips to form a 50-Å-adhesion layer prior to additional evaporation of the actual metal under examination. The evaporation rate from the source (N) is calculated based on the deposition rate:

$$N = \frac{R_D 4\pi r^2 D N_A}{A_s M_s} \left[ \frac{\text{molecule}}{\text{cm}^2 \cdot \text{s}} \right] \quad (1)$$

where:

- $R_D$  is the deposition rate (Å/s) at the substrate
- $D$  is the density of the source
- $N_A$  is Avogadro's number
- $M_s$  is the molecular weight of the evaporant
- $A_s$  is the surface area of the source

A deposition rate of chrome at 5 Å/s corresponds to a value of  $4.15 \times 10^{15}$  atoms/cm<sup>2</sup>·sec impinging on the substrate. 100 Å of the metal used for biomolecular adhesion is subsequently deposited onto the chrome layer at rates of 10 Å/s for gold ( $5.89 \times 10^{15}$  atoms/cm<sup>2</sup>·sec), Cu ( $8.46 \times 10^{15}$  atoms/cm<sup>2</sup>·sec), and 5 Å/s Ni ( $4.55 \times 10^{15}$  atoms/cm<sup>2</sup>·sec). Special care is taken to minimize corrosion and oxidation of the Cu substrates. Thus, Cu substrates are stored under vacuum prior to experimentation.

Continuing with the above example, a synthetic peptide containing a six His-tag (NH<sub>2</sub>-Gly-Gly-Lys-Gly-Gly-Lys-Gly-Gly-His-His-His-His-His-His-CO<sub>2</sub>H) is covalently coupled to carboxylate-modified 2 and 10 μm fluorescent microspheres (Molecular Probes, Eugene, OR) using a water-soluble carbodiimide. Alternative affinity tags, including cysteine and proline, are of potential use for attachment. A 50-μl aliquot of His-tagged microspheres are allowed to attach to glass, nitrocellulose, gold-, copper-, and nickel-coated coverslips for 2-15 minutes at room temperature (FIG. 5). Unattached microspheres are removed through a series of washes, and coverslips

are observed using fluorescence microscopy. The bond strengths between His tagged-microspheres and gold, copper, and nickel substrates are evaluated using high velocity laminar flow. His-tagged microspheres attach to all three substrates; however, the attachment is greatest on the nickel-coated coverslips.

A custom fabricated flow-cell consisting of fluid input/output and vacuum ports is used to mount the substrates, and apply a variable fluidic flow across the surface. The laminar flow system is essentially a machined, polished Lucite™ block (Immunetics, Inc., Cambridge, Ma., Model CAF-10). The substrates are secured in a rectangular recess in the flow-cell. Consequently, the equations for rectangular channel and open-duct geometry are used for fluid flow analysis. A continuous vacuum is applied during tests to keep the coverslips from shifting as water enters the flow chamber. Fluidic flow is observed with live imaging. The imaging system consists of a stereo-microscope (Leica, Inc., Deerfield, Ill., Model Wild M3Z) attached to a Photometrics video camera and accompanying Photometrics video capture computer software. A 50x working distance magnification provides the required resolution to observe the fluorescent microspheres on the substrates on the computer. Images are taken with the CCD camera and transmitted to the computer's video capture board for processing. A circular field of view is established to obtain an accurate estimate of microsphere attachment and removal.

A direct-drive infusion pump provides laminar fluid flow, and microsphere removal is observed at each flow rate. The flow rate is controlled using an infusion pump equipped with a 60-ml syringe filled with deionized water. The entire system is placed on a vibration isolating laboratory platform (Newport Dcorp., Irvine, CA).

Prior to actual testing, all input/output lines and valves are purged of air bubbles introduced in between experiments during substrate removal, cleaning, and syringe refill. Several milliliters of water are discharged by gravity head through the system to completely fill the test chamber, and once the absence of air bubbles and the stability of flow across the substrates are verified, examinations of substrate adhesion strength are initiated.

The flow rate of water flowing through the system is determined by collecting the fluid from the output port at timed intervals. Variable fluidic flow is controlled through two rheostat adjustments on the pump—one for the % speed control (ranging

from 0 to 130 percent) and one for infusion rate control (neutral to 9). The highest flow setting, 130% speed control and a rate setting of 1, is reserved mainly for Ni substrate testing and complete microsphere removal evaluations for the other substrates.

The overall flexibility in pump flow settings provides the necessary range of flow rates to generate a broad distribution of data points, and thereby help evaluate the point of adhesion force disruption for the various coated coverslips. Results are obtained and recorded from 5 replicate trials with each substrate to ensure precision and reproducibility of data and to examine distribution errors of force assessments.

To calculate the force required to disrupt microsphere adhesion, the number of microspheres within the field of view is determined for each timed interval (1 to 5 minutes) and flow rate (0 to 52 ml/min). Navier-Stokes equations representing three dimensional flow through rectangular ducts are utilized to estimate the velocity of flow at 5- $\mu$ m above the substrate:

$$u_z = (u_c + u_p)_z \quad (2)$$

Where  $u_c$  and  $u_p$  are the respective complementary and particular parts of the velocity equation in the z (vertical)-direction.

The complementary solution is approximated with an infinite series (with  $n = 0$  to 1000) of the form shown below in equation 3. In addition, equation 4 defines the particular solution. Note that the hydraulic gradient  $dp/dx$  (that appears in both equations 3 and 4) is defined by flow cell geometry and flow rate, and is expressed in equation 5.

$$u_c(z) = \frac{\sum_{n=1}^{1000} \frac{2B^2}{\mu} \frac{dp}{dx} \left( \alpha_n \cos \frac{\alpha_n}{2} - 2 \sin \frac{\alpha_n}{2} \right) \cos \left( \frac{(2n-1)\pi z}{2B} \right) \cosh \left( \frac{((2n-1)\pi x)}{2B} \right)}{\alpha_n^3 \cosh \left( \frac{(2n-1)\pi W}{4B} \right)} \quad (3)$$

$$u_p(z) = \frac{1}{2\mu} \left( \frac{dp}{dx} \right) \left( \frac{B^2}{4} - Z^2 \right) \quad (4)$$

$$dp/dx = 1.5 Q\mu/B^3W = 6.22 \times 10^5 \cdot Q \quad (5)$$

where:  $\mu$  = kinematic viscosity of water [gm cm/sec]  
 $dp/dx$  = change in pressure head per unit length of the flow cell  
 $x$  = distance along the fluid flow direction from the midpoint of the cell [cm]  
 $y$  = distance along the orthogonal direction of flow from the centerline cell but within the same plane of the flow field [cm]  
 $z$  = vertical distance from the substrate in the flow field  
 $Q$  = flow rate [cm<sup>3</sup>/sec] (in this case along the x direction)  
 $B$  = height of the flow cell (measured to be 0.016 cm)  
 $W$  = flow cell width (0.559 cm)

The kinematic viscosity of water varies between experiments over the range of 0.890 to 1.139 gm/cm•sec (corresponding to 15 to 25 degrees C, respectively) and is estimated with a linear equation relating  $\mu$  with temperature (22.4°C):

$$\begin{aligned}\mu &\equiv 1.51 - 0.025T & (6) \\ &= 1.51 - (0.025 \cdot 22.4) \\ &= 0.95 \text{ gm/cm}\cdot\text{sec}\end{aligned}$$

The value of  $z$  that appears in the complementary and particular velocity equations (3 and 4) is defined for this particular flow test application to be 0.0005 cm (the radius of the 10-micron fluorescent beads used in experimentation). Ultimately, evaluating the expressions for the complimentary and particular solutions yields:

$$\begin{aligned}u_c &= -4.195 \times 10^{-15} \cdot Q \\ u_p &= 20.880 \cdot Q\end{aligned}$$

With the above estimates for the components of the velocity equation, the shearing stress is calculated using Stokes law for laminar flow against stationary particles bound to substrates within the test channel:

$$F = 6\pi\mu(u_c + u_p)r \quad (7)$$

where:  $F$  represents the force in nano-Newtons (nN)  
 $r$  is the radius of microsphere (5- $\mu$ m)  
 $\mu$  represents kinematic viscosity

Equation (7) is valid only in laminar flow conditions which is verified by calculating the Reynolds number to ensure that it is less than 1000:

$$Re = \frac{Q\rho}{B\mu} \quad (8)$$

in which  $\rho$  is the density of water and the other terms are the same as those appearing in the aforementioned equations. Accordingly, at a test condition of 22.4°C and flow rates less than 5 ml/sec (the maximum obtainable infusion rate with the pump is 0.867 ml/sec), laminar flow is maintained in the system and Stokes law provides sufficient approximations of shear forces. Equation 6 is also used for determining what is designated as " $F_{r66}$ " or the force required to remove approximately 66% of the original number of microspheres appearing in the field of view. This estimate offers an informative, quantifiable means of comparing substrate-binding strengths.

To test the strength of attachment, laser tweezers are used to remove the microspheres from the substrate. The laser tweezers, however, are unable to remove microspheres from any of the three substrates suggesting that the bonding strength was greater than 600 pN. Further attempts to remove the microspheres with high velocity flow suggest that the bonding strength increases from gold to unoxidized copper to nickel. Oxidized copper does not serve as a suitable surface for binding of His-tagged microspheres (Soong *et al.*, 1999).

The force required to remove 66% of the microspheres ( $F_{r66}$ ) from a substrate further demonstrates the differences among the various media (Table 1). The  $F_{r66}$  for each substrate is determined by locating the intersection point at 66% removal. Glass and gold possesses relatively similar  $F_{r66}$  values (Table 1). Van der Waals interactions account for the comparatively weak binding of the microspheres to the gold surface.

Substrate Type	Calculated $F_{r66}$ (nN)
Glass	53
Nitrocellulose	75
Gold	41
Copper	150
Nickel	>160

Table 1: Shear force ( $F_{r66}$ ) required to remove 66% of the His-tagged microspheres attached to the various substrates.

The  $F_{r66}$  increases from nitrocellulose, to unoxidized copper, to nickel (Table 1). Nitrocellulose slides exhibit a higher  $F_{r66}$  than gold, which may be attributed to the uneven surface of the nitrocellulose-coated slides and the charged, dipole-dipole interactions between the nitrocellulose molecules and the fluorescent microspheres. The exact  $F_{r66}$  of nickel is not determined because only a small percentage (<1.32%) of microspheres are removed at the maximum flow rate attainable with this system. Greater flow rates are required to accurately evaluate the bonding strength properties and capabilities of nickel media.

Together, these experiments demonstrate a chemical mechanism for attaching biological molecules to substrates. The metals utilized in this study are widely used in nanofabrication, and possess a range of affinity for biological molecules. Using this knowledge in conjunction with standard and novel electron beam lithographic methods, proteins can be attached to metallic substrates with precise orientation, positioning, and spacing.

The confluence of molecular biology and nanofabrication provide, for the first time, the ability to create hybrid organic/inorganic NEMS. These devices provide a means for the seamless integration of NEMS with living systems. Imagine a NEMS device powered by a cell's own energy which is capable of pumping fluids across cell membranes. Further, imagine the biomolecular motors of the same NEMS device being continually replaced by the cell as their function ceases. Only human innovation and imagination limit the application and evolution of such devices.

Precise positioning and orientation of single molecules are essential to the development of hybrid NEMS devices. Patterned arrays of nickel dots (20-100 nm diameter, 1  $\mu$ m spacing) are constructed on coverslips using electron beam lithography.  $F_1$  ATPase molecules are attached to these patterned arrays through the His tags on the

$\alpha$  and/or  $\beta$  subunits. Individual  $F_1$ ATPase molecules attach to the nickel dots as demonstrated by atomic force microscopy of the nickel arrays before and after attachment of  $F_1$ ATPase molecules. Fluorescent microspheres are then attached to the tip of the  $\gamma$  subunit using a streptavidin-biotin linkage to demonstrate the spacing and orientation of the individual molecules. The ability to precisely locate these molecules is achieved in the X, Y and Z dimensions. The ability to attach single biological molecules with precise spacing, location, and orientation using nanofabricated substrates is demonstrated.

Although the biological and chemical aspects of  $F_1$ -ATPase have been studied, relatively little is known about the engineering properties of this enzyme. Therefore, an evaluation of  $F_1$ -ATPase performance as a molecular motor in hybrid NEMS devices is necessitated. Analysis of crystallized  $F_1$ -ATPase suggests that the  $\gamma$  subunit is displaced from the central axis during rotation a distance  $>20 \text{ \AA}$  (Bianchet *et al.*, 1998). By attaching a  $1 \text{ }\mu\text{m}$  microsphere to the  $\gamma$  subunit, the displacement and angle of deformation of the  $\gamma$  subunit can be determined by measuring the radial displacement of the microsphere. The angle of deformation will provide valuable insight on the mechanism behind rotation of the  $\gamma$  subunit. Further, the exact path and eccentricity of rotation must be determined in order to create useful NEMS devices.

The  $\gamma$  subunit of the recombinant  $F_1$ -ATPase is specifically biotinylated through disulfide linkage to the  $\gamma$ Cys. By using the newly developed attachment system described above, the biotinylated protein then is attached to an array of 30 nm gold dots deposited on a coverslip. Fluorescent  $1 \text{ }\mu\text{m}$  microspheres coated with streptavidin are allowed to bind to the biotinylated  $\gamma$  subunits (FIG. 4).

Subsequently, unattached microspheres are removed through a series of washes. Rotation of the  $\gamma$  subunit is initiated by the addition of  $2 \text{ }\mu\text{M}$   $\text{Na}_2\text{ATP}$  in presence of  $4 \text{ }\mu\text{M}$   $\text{MgCl}_2$ . Movement of the microsphere is measured using a differential interferometer (Denk and Webb, 1990; Stelick *et al.*, 1999). Images of microsphere movement are also captured at 1 msec intervals using the CCD kinetics camera.

Initially, the interferometer is calibrated using His-tagged microspheres attached to nickel slides. Microsphere movements as small as 5nm with a resolution

less than 1 nm are detected by the interferometer. For the expected range of translation ( $<75$  nm), the measured normalized voltage is a linear function of microsphere displacement. Further examination, however, indicates that changes in voltage are a function of both the direction and the magnitude of displacement. A series of calibration curves are calculated for microsphere displacement at angles between 0 and  $90^\circ$ , which clearly illustrate that both distance and angle of displacement affect the response of the instrument. Therefore, a quadrant detector is added to measure the angular direction of the microsphere's movement, and permit an accurate quantification of the real-time deformation of the  $F_1$  ATPase protein during ATP catalysis.

The quadrant detector is calibrated for determining the angle of displacement. Experiments are performed for angles between 0 and  $360^\circ$  and distances between 65 and 150 nm. These data are used to produce an equation by which voltage changes (interferometer) and angle measurements (quadrant detector) are translated in accurate measures of displacement. This equation is used to accurately measure the displacement of a microsphere attached to the  $\gamma$  subunit of  $F_1$ ATPase.

Initial tests to evaluate the rotation of the  $\gamma$  subunit are performed using the assay described above. Interferometer data demonstrates microsphere movement at approximately 9.5-10.5 Hz. Following the assumption that the  $\gamma$  subunit moves in three,  $120^\circ$  steps, the rotation of the  $\gamma$  subunit is approximately 3-4 r.p.s. Measurements of the background, as well as a microsphere in the absence of ATP display no signal using the interferometer. Similar results are obtained when  $1\ \mu\text{m}$  streptavidin-coated magnetic microspheres are attached to the  $F_1$ -ATPase.

Image analysis demonstrates that microsphere movement occurs in three discrete steps following a counterclockwise pattern at a rate of approximately 3-4 r.p.s. The data confirm a counterclockwise, three step rotational mechanism of hydrolysis previously reported by Yashuda *et al.* (1998).

Microsphere movement ceases approximately 40 minutes following the initial addition of ATP. Prior to stopping, microspheres remain at rest for periods up to approximately 600 msec, followed by 500 msec of continuous movement. This pattern of movement is attributed to low concentration of ATP in solution.

Continuous movement is reinitiated following the addition of fresh ATP to the flow cell, suggesting that movement of the microsphere (rotation of the  $\gamma$  subunit) are dependent upon the presence of ATP.

These experiments demonstrate a chemical mechanism for protein binding and positioning to engineered structures that are compatible with current nanofabrication technologies. Using this knowledge in conjunction with standard e-beam lithographic methods (Craighead and Mankiewich, 1982; Lercel *et al.*, 1995; Lercel *et al.*, 1996; Carr and Craighead, 1997) individual motor protein molecules can now be attached with a precision greater than 20-30 nm.

The objective is to develop a technology to power implantable prosthetic, diagnosis and drug delivery systems that uses the physiology of the patient to power and maintain the device. This effort is the first step toward the seamless integration of nanoscale technologies with living systems. Despite the superb performance of the  $F_1$ -ATPase motor protein, successful application of the enzyme to mechanically pump fluids and open and close valves in microfluidic devices will require forces on the order of 10's of nN. This is at least a factor of 100 greater than can be provided by a single motor. Consequently, successfully extracting useful mechanical power from the  $F_1$ -ATPase motor will most likely require being able to couple the power of an array of motor proteins to a desired hybrid device.

#### Using Light to Power Hybrid NEMS Devices

A major problem regarding the integration of biomolecular motors with NEMS devices revolves around the ability to maintain the fuel source for the motor. When considering the application of such devices within a living cell, the fuel source (i.e., ATP) can be supplied by the host cell. However, a system of maintaining the fuel source for autonomous hybrid NEMS devices must be constructed. An embodiment of the invention includes such a fuel source.

Bacteriorhodopsin (BR) is a membrane-bound protein originally isolated from the purple membranes of *Halobacterium halobium* (Vsevolodov, 1998). BR utilizes solar radiation to translocate protons outwards, forming an external proton gradient.

Subsequently, the  $F_0F_1$ -ATPase complex utilizes the gradient to pump the protons into the cell, and synthesizes ATP (Vsevolodov, 1998; Nicholls and Ferguson, 1992). Formation of the purple membrane and BR are light dependent processes. The absorption spectra of BR ranges from 400 to 700 nm, with a peak absorbency at approximately 580 nm.

Artificial systems consisting of BR and  $F_0F_1$ -ATPase complexed in liposomes have been used to demonstrate the light driven production of ATP (Richard *et al.*, 1995; Pitard *et al.*, 1996a, 1996b). A liposome is a vesicle composed of one or more concentric phospholipid bilayers which is used medically especially to deliver a drug into the body. In these systems, BR pumps protons from the surrounding media into the artificial liposomes. The internal gradient then is utilized by  $F_0F_1$ -ATPase to translocate protons back across the liposome membrane, and synthesize ATP external to the liposome (FIG. 6). ATP production rates of up to 700 nmol ATP/min/mg  $F_0F_1$ -ATPase have been reported (Pitard *et al.*, 1996a). This system provides an efficient mechanism by which solar radiation leads to the production of ATP. The light-driven ATP production system is well suited for maintaining a fuel source (i.e., ATP) in hybrid devices.

Nanoscale, engineered systems that harness light energy to perform mechanical work are demonstrated here. Artificial liposomes comprised of reconstituted  $F_0F_1$ -ATP synthase and bacteriorhodopsin are used to synthesize ATP (Richard *et al.*, 1995; Pitard *et al.*, 1996a). Subsequently, the ATP is used to provide energy to power a recombinant, thermostable  $F_1$ -ATPase biomolecular motor that is coupled to a NEMS device.

Recent research has clearly demonstrated that ATP can be produced via photosynthetic processes from liposomes comprised of  $F_0F_1$ -ATPase and either BR (Richard *et al.*, 1995; Pitard *et al.*, 1996a, 1996b) or artificial chlorophyll (Steinberg-Yfrach *et al.*, 1998). Results of these studies illustrate that sufficient quantities of ATP can be produced in an environment which is consistent with the requirements of  $F_1$ -ATPase powered NEMS. Thus, the integration of a similar system with the biomolecular motor-powered systems described herein is described.

The application of light-driven ATP production system to power a hybrid NEMS device is discussed below. Optimal rates of ATP production (500-700 nmol/min/mg  $F_0F_1$ -ATPase) are achieved when a single  $F_0F_1$ -ATPase is embedded in liposomes composed of phosphatidylcholine, phosphatidic acid, and cholesterol.

Using these figures, the number of liposomes required to power a single  $F_1$ -ATPase biomolecular motor integrated in a NEMS device are calculated (FIG. 7). These figures are calculated for an equilibrium situation in which the  $F_1$ -ATPase motor is continuously being supplied with ATP. Since the exact number of  $F_1$ -ATPase motors attached to a substrate can be determined, the number of liposomes present in the solution can be manipulated to satisfy the expected demand. Therefore, ATP can be overproduced by varying the number of liposomes in this system to provide an excess fuel source during periods lacking solar radiation.

In addition to the number of liposomes required, the length of one side of a light harvesting device necessary to provide adequate ATP production to keep a hybrid NEMS device at equilibrium has been calculated (FIG. 8). This size varies from as small as 87 nm to approximately 1.15  $\mu$ m in size. The complementation of these two variables (i.e., number of liposomes and length of one side of a light harvester), establishes the minimum dimensions of a hybrid NEMS device that is powered by solar radiation.

Based upon the calculations, the BR-ATPase containing liposomes represent an excellent means for maintaining continuous supply of ATP for a hybrid biomolecular motor-powered NEMS device. The integration of this system with the current  $F_1$ -ATPase powered NEMS device described herein demonstrates the capability of creating an autonomous, light powered NEMS device. The applications of such devices, as well as the subsequent evolution of this technology, open the door the creation of novel classes of useful NEMS devices.

A system for the light dependent production of ATP, and the continuous maintenance of the fuel supply for a hybrid NEMS device is described. As a means for fueling  $F_1$ -ATPase-powered NEMS devices, artificial liposomes containing

bacteriorhodopsin and  $F_oF_1$ -ATPase are constructed by technique known in the art, and incorporated by reference (Pitard *et al.*, 1996a; Richard *et al.*, 1995).  $F_oF_1$ -ATPase is isolated from *Bacillus* PS3 (Matsui and Yoshida, 1997), and bacteriorhodopsin is isolated as described by Oesterhelt and Stoerkenius (1974). The  $F_oF_1$ -ATPase is reconstituted in liposomes containing bacteriorhodopsin (Pitard *et al.*, 1996a). The present invention provides a unique, novel system wherein ATP synthesis is evaluated under conditions relevant to subsequent integration in hybrid NEMS devices.

The light energy is collected in liposomes that are approximately 150 nm in diameter. Bacteriorhodopsin (BR) and  $F_oF_1$ -ATPase are incorporated into the membrane of the liposome. As light strikes the liposome, BR translocates protons across the membrane, and produces a high concentration of protons within the liposome. The resulting proton gradient provides the proton motive force for the production of ATP by  $F_oF_1$ -ATPase. The produced ATP then is used as fuel by an engineered  $F_1$ -ATPase biomolecular motor coupled with a NEMS device. The waste products from this reaction (i.e., protons, ADP, and inorganic phosphate) are recycled through the liposome's ATP production cycle, resulting in closed chemical system. Constructing an integrated system such as this results in the ability to produce autonomous light powered hybrid NEMS.

The NEMS device construct are composed of two separate components: (1) ATP-producing liposomes and (2) hybrid NEMS devices. This device serves as a model system for studying and characterizing the performance of the biomolecular motor activity/ATP production unit. A device must be built that facilitates direct quantitative observation of the activity of the molecular motors and liposomes, is relatively easy to assemble and is amenable to system design modifications.

The first step in constructing the NEMS device is to construct the ATP-producing liposomes. Systems for the production of light-driven ATP production using bacteriorhodopsin and liposomes have previously been established by the said technique being known in the art, and incorporated by reference (Richard *et al.*, 1995; Pitard *et al.*, 1996a, 1996b). A similar system is constructed and characterized. This ATP production system is then incorporated into a hybrid device.

The second step in constructing the NEMS device is producing the  $F_1$ -ATPase-powered hybrid system. A patterned array of nickel dots is prepared on 25mm diameter round coverslips using electron beam lithography (Montemagno and Bachand 1999). The array contains a square grid (25 x 25) of nickel dots (~25 nm) equally spaced at 5  $\mu$ m intervals in both dimensions. Biotinylated  $F_1$ -ATPase motors are attached to the nickel array through the His-tags on the  $\alpha$  and  $\beta$  subunits. Subsequently, streptavidin-coated microspheres (1-2  $\mu$ m) are attached to the  $\gamma$  subunit through the streptavidin-biotin linkage (FIG. 9). Excess microspheres and  $F_1$ -ATPase are removed through a series of washes.

The final step in creating the device involves the integration of the two components (FIG. 9). By using a patterned array to attach the  $F_1$ -ATPase molecular motors, the maximum number of motors per device can be predetermined. Therefore, the number of liposomes required to keep the hybrid system in equilibrium can be calculated using FIG. 7. Assuming all the nickel dots are occupied with  $F_1$ -ATPase motors (625 total), approximately 2350 liposomes are required to keep this system at equilibrium (assuming ATP production = 500 nmol ATP/min/mg  $F_0F_1$ -ATPase, and rotational velocity of the motor = 5 r.p.s.). These numbers are conservative estimates based upon previous findings with both systems (Richard *et al.*, 1995; Pitard *et al.*, 1996a, 1996b; Montemagno and Bachand 1999). The device is integrated using a flow cell system previously described (Montemagno and Bachand, 1999). The coverslip is mounted on the piezo-stage, and a solution containing the liposomes, ADP, and Pi are infused into the flow cell. An external light source is applied to the system to initiate ATP production by the liposomes. Following a lag period, the level of ATP reaches a concentration at which it begins to power the  $F_1$ -ATPase – microsphere device. The activity of the biological motors are monitored using a differential interferometer and quadrant detector (Montemagno and Bachand, 1999). These data allow for accurate and precise determination of the rotational velocity of the  $F_1$ -ATPase motor.

Once baseline data are collected for this system, a number of experiments are conducted to evaluate its performance. The effect of varying liposome number are evaluated in relation to  $F_1$ -ATPase motor performance. For example, the number of

liposomes are added at a two-fold excess (~4700 liposomes/625  $F_1$ -ATPase motors). Based upon the calculations, doubling the number of liposomes should permit the motor to run in the absence of light for a period equal to the length of time that the device was exposed to an external light source. The effect of increasing liposome number by factors of 3-, 4-, 5-, and 10-fold are examined. To date, virtually nothing is known about the "life span" of the  $F_1$ -ATPase motor, the ATP-producing liposomes, and the integrated system. Thus, the sustainability over periods of time are also examined. These investigations can then be expanded to evaluate the effect that environmental factors such as temperature and pH variations have on the performance and stability of the system.

After the basic dynamic of the biomolecular motor/ATP production dynamics are established, engineering issues associated with the fabrication of useful engineering devices can be explored. Central to this is the design of compartmentalized devices in which the ATP production portion of the system is isolated from the "work" function of the device. This requires the development of selectively porous chambers that permit the ready diffusion of ATP, ADP and inorganic phosphate yet isolate the liposomes from the NEM functions. Consequently, the previously described device is modified to incorporate chambers constructed with various materials (porous silicon, organic and inorganic polymers etc.) and different geometries. Thus issues associated with material selection and chamber geometry and their associated affects on chemical diffusion and overall system performance are also studied.

This embodiment of the invention creates a system for the continuous supply of fuel for a hybrid, biomolecular motor-powered NEMS device. To demonstrate the feasibility and application of such a system, the worlds first photosynthetic powered,  $F_1$ -ATPase driven NEMS device (FIG. 9) is described. Once the platform for integrating these separate systems (i.e., ATP producing liposomes and  $F_1$ -ATPase powered NEMS devices) is established, novel types of autonomous NEMS devices capable of harnessing useful work from biomolecular motors can be created.

### Creating an "on/off switch" for F<sub>1</sub>-ATPase

The use of ATP powered biological motors establishes the opportunity to develop autonomous devices that are maintained and fueled by the physiology of a host organism. Mechanisms for controlling the motor, however, must be instituted in order to fully successfully employ this technology. Thus, this aspect of the invention establishes the necessary foundations for controlling biomolecular motor-powered devices. A recombinant F<sub>1</sub>-ATPase motor protein is modified such that its activity can be controlled by a chemical signal. Subsequently, a hybrid nanomechanical system powered by this modified motor is constructed (FIG. 10).

To control motor activity, the F<sub>1</sub>-ATPase must be modified such that its function can be controlled by an environmental factor (i.e., environmentally controlled switch). In its native state, the F<sub>1</sub>-ATPase protein possesses three ATP binding sites located on the  $\alpha$  subunit. The three  $\beta$  subunits, in turn serve as the catalytic sites for ATP synthesis/hydrolysis. By engineering a new affinity binding site into the protein, this site can prevent conformation changes necessary for the catalysis of ATP when the new site is occupied.

The mechanism of ATP synthesis/hydrolysis recently has been examined using protein crystallography (Bianchet *et al.*, 1998). In order for ATP synthesis/hydrolysis to occur, all three sites of F<sub>1</sub>-ATPase are occupied as follows: ADP (closed, C), ADP + P<sub>i</sub> (loose, L), and ATP in equilibrium with ADP + P<sub>i</sub> (tight, T). During ATP synthesis, conformational changes initiate an ordered transformation of the subunits: T to C, L to T, and C to L (Bianchet *et al.*, 1998). Subsequent to these changes, one ATP molecule is released and the  $\gamma$  subunit rotates 120° about its axis. During ATP hydrolysis, these series of changes are reversed (i.e., L to C, T to L, and C to T).

To control the activity of the motor, the  $\alpha$  and  $\beta$  subunit coding sequence are modified in order to form an additional affinity binding site. When occupied, this binding site stabilizes the interface between the  $\alpha$  and  $\beta$  subunit thus preventing the conformational changes necessary for ATP hydrolysis. To create this new binding site, two amino acid residues on the  $\beta$  subunit and one amino acid residue on the  $\alpha$  subunit are

changed to His. When the protein is properly assembled and folded, these three His form a metal binding site that will efficiently bind zinc. This zinc-binding pocket prevent the subunits from making conformational changes necessary for ATP hydrolysis, thereby turning the motor "off". To restore the motor's activity and turn the motor back "on", zinc is removed through the addition of EDTA.

Selection of the binding site is done through a combination of analysis of the crystallographic structural data and molecular modeling. By preparing a double distance map that examines the distance changes between residues during the transition of the catalytic site from open to loose to tight, residue pairs which exhibit a large conformation change during synthesis/hydroloysis and possess the proper relative conformational relationship can be identified. The molecular modeling program Dezymer (Hellenga, 1998) is used to evaluate the effect of changing the identified residues to Histidines. This provides a set of possible locations for inserting the metal binding site.

Site directed mutagenesis is used to modify the  $F_1$ -ATPase coding sequence to create the zinc-binding pocket. The "working" clone (pGEM-MH) of the  $F_1$ -ATPase from the thermophilic bacterium, *Bacillus* PS3 described above can be used as the starting point for these mutagenesis studies. The sequence changes to the  $\alpha$  and  $\beta$  subunits are made using this clone. Subsequently, the modified sequence is subcloned into pQE-30 for expression of the recombinant protein. Expression and purification is carried out as described above.

The modified  $F_1$ -ATPase switch is tested using an ATP regeneration assay previously described (Matsui *et al.* 1997; Matsui and Yoshida 1995). Initially, the activity of the native and modified  $F_1$ -ATPase is compared in the absence of zinc. Following baseline performance measurements, various concentrations of zinc (100  $\mu$ M to 100 mM) are used to turn the switch "off," and the activity measured. Various concentrations of EDTA (100  $\mu$ M to 100 mM) are also used to turn the motor "on," and ATPase activity again is measured. In addition to varying concentrations of zinc and EDTA, assays are conducted at temperatures ranging from 20 to 75°C (optimal activity for the native  $F_1$ -ATPase is 65°C). Varying temperatures provide insight to the binding

strength of zinc to the Histidine pocket. A series of modified  $F_1$ -ATPase motors with the zinc binding sites in different locations are produced until a "switch" with acceptable performance is developed.

Once the activity of the modified  $F_1$ -ATPase is determined, the motor can be integrated into a hybrid system. Nanofabricated substrates to position the motor with precise spacing and orientation are utilized. Control of the motor activity is assayed using a reporter molecule attached to the  $\gamma$  subunit of  $F_1$ -ATPase.

To visually examine the efficacy of the switch, an ATPase-powered hybrid system is created. The modified  $F_1$ -ATPase is specifically biotinylated through disulfide linkage to the Cys located at the tip of the  $\gamma$  subunit. Subsequently, the biotinylated motor is attached to a patterned nickel array deposited on a coverslip. Streptavidin-coated microspheres (1  $\mu\text{m}$ ) are attached to the  $\gamma$  subunit through the streptavidin-biotin linkage.

The  $F_1$ -ATPase powered hybrid system is controlled through the addition of zinc, followed by chelation with EDTA (FIG. 11). Rotation of the  $F_1$ -ATPase hybrid system is initiated (switch on) by the infusion of an ATP regeneration solution described in Yashuda *et al.*, 1998. Rotational velocity and angle of deformation of the microspheres can be measured using a differential interferometer and quadrant detector, respectively. Rotation is stopped (switch off) by infusion of the ATP regeneration solution containing zinc (concentration having been determined using the activity assays described above). Microsphere movement is recorded using the interferometer and quadrant detector. Rotation is re-initiated (switch on) by the infusion of an ATP regeneration solution containing EDTA (concentration having been determined using activity assays described above). Rotational velocity and angle of deformation again is measured using the interferometer and quadrant detector. These steps are repeated to determine the number of times that the  $F_1$ -ATPase system can be turned on and off without affecting motor performance.

Once baseline data has been collected on the hybrid system, varying concentrations of zinc and EDTA can be examined in relation to their effects on

switching and motor performance. In addition, the effect of temperature can be examined. These data provide a strong foundation for understanding how a biomolecular motor-powered system can be controlled by an environmental factor. In addition, these technologies open the door for the creation of a novel class of biomolecular motor-powered hybrid devices that can be controlled by external stimuli such as temperature and chemical signals.

Establishing mechanisms for controlling biomolecular motor-powered devices allows for the creation of novel classes of NEMS which can be seamlessly integrated with living systems. For example, biological sensors (biosensors) can be created by modifying the biomolecular motor such that its activity is inhibited, or stimulated, in the presence of an external stimulus (e.g., chemical, thermal, etc.). Imagine analyzing an environmental sample by simply applying a portion to a NEMS device in which thousands of biomolecular motors had been modified to contain binding sites for an array of different chemicals. NEMS devices also could be used for delivery of pharmaceutical agents to specific cell types, chemical agents, environmental agents, or sites by engineering biomolecular motors to recognize cell-specific signals. The limitations of controllable biomotor-powered NEMS devices are bound only by human imagination and innovation.

#### Applications for NEMS hybrids

Current applications being developed include nanite "scrubbers" designed to scrape plaque from the interior walls of arteries, drug dispensing "systems" on a microchip. The types of components to be coupled to the  $F_1$ -ATPase molecule include sensors, mechanical actuators, pumps, propulsion devices, micro electronic circuitry. Even though these NEMS are coupled to an organic molecule including at least one  $F_1$ -ATPase molecular motor biocompatibility is of extreme importance for implantable micro systems. To ensure the required level of biocompatibility organic molecules in addition to the  $F_1$ -ATPase motor may need to be applied to the surface of the silicon-based components to shield them from detection by an implanted organism's immune system.

Accordingly, it is to be understood that the embodiments of the invention herein described are merely illustrative of the application of the principles of the invention. Reference herein to details of the illustrated embodiments are not intended to limit the

scope of the claims, which themselves recite those features regarded as essential to the invention.

What is claimed is:

- 1 1. A method of attaching at least one protein to a substrate comprising:
  - 2 a) fabricating a first pattern of molecules onto a first site specific location on  
3 said substrate;
  - 4 b) genetically engineering a first molecular support onto a first protein such  
5 that said first molecular support is capable of binding to said first pattern  
6 of molecules; and
  - 7 c) binding said first pattern of molecules to said first molecular support such  
8 that said first protein is attached to said first site specific location on said  
9 substrate.
- 1 2. The method of claim 1 further comprising:
  - 2 d) fabricating a second pattern of molecules on a second site specific location on  
3 said substrate;
  - 4 e) genetically engineering a second molecular support onto a second protein  
5 such that said second molecular support is capable of binding to said  
6 second pattern of molecules; and
  - 7 f) binding said second pattern of molecules to said second molecular support  
8 such that said second protein is attached to said second site specific  
9 location on said substrate.
- 1 3. The method of claim 2 wherein said first site specific location and said second site  
2 specific location are in sufficient proximity such that said first protein and said  
3 second protein can operatively associate to perform sequential enzymatic  
4 reactions.
- 1 4. The method of claim 1 wherein said first molecular support comprises an affinity tag.
- 1 5. The method of claim 1 wherein said first molecular support comprises a histidine tag.

- 1    6. The method of claim 1 wherein said first pattern of molecules comprises a metal.
- 1    7. The method of claim 6 wherein said first pattern of molecules is selected from the  
2        group consisting of:
  - 3            a) nickel;
  - 4            b) copper;
  - 5            c) iron; and
  - 6            d) gold.
- 1    8. The method of claim 1 wherein said first pattern of molecules is comprised of a  
2        polymer.
- 1    9. The method of claim 1 wherein said first pattern of molecules is comprised of a  
2        composite with a binding affinity for an enzymatic tag.
- 1    10. A combination of at least one protein and a substrate comprising:
  - 2            a) said substrate including a first pattern of molecules fabricated onto a first site  
3                specific location on said substrate; and
  - 4            b) a first protein including a first molecular support genetically engineered into  
5                said first protein that is bound to said first pattern of molecules.
- 1    11. The combination of said at least one protein and said substrate of claim 10 further  
2        comprising:
  - 3            c) a second pattern of molecules on a second site specific location on said  
4                substrate; and
  - 5            d) a second protein including a second molecular support genetically engineered  
6                into said second protein that is bound to said second pattern of  
7                molecules.

- 1 12. The combination of said at least one protein and said substrate of claim 11 wherein  
2 said first site specific location and said second site specific location are in  
3 sufficient proximity such that said first protein and said second protein can  
4 operatively associate to perform sequential enzymatic reactions.
- 1 13. The combination of said at least one protein and said substrate of claim 10 wherein  
2 said first molecular support comprises an affinity tag.
- 1 14. The combination of said at least one protein and said substrate of claim 10 wherein  
2 said first molecular support comprises a histidine tag.
- 1 15. The combination of said at least one protein and said substrate of claim 10 wherein  
2 said first pattern of molecules comprises a metal.
- 1 16. The combination of said at least one protein and said substrate of claim 15 wherein  
2 said first pattern of molecules is selected from the group consisting of:  
3 a) copper;  
4 b) nickel;  
5 c) iron; and  
6 d) gold.
- 1 17. The combination of said at least one protein and said substrate of claim 10 wherein  
2 said first pattern of molecules is comprised of a polymer.
- 1 18. The combination of said at least one protein and said substrate of claim 10 wherein  
2 said first pattern of molecules is comprised of a composite with a binding  
3 affinity for an enzymatic tag.
- 1 19. A nanoscale engineered system comprising at least one nano-electro-mechanical  
2 system wherein said nano-electro-mechanical system is operatively connected to  
3 and harnesses mechanical motion of a portion of at least one chemical enzyme  
4 that undergoes a conformational shift.

- 1 20. The nanoscale engineered system of claim 19 wherein said portion of at least one  
2 chemical enzyme is a portion of an ATP synthase complex.
- 1 21. The nanoscale engineered system of claim 19 wherein an attachment between said  
2 portion of at least one chemical enzyme and said at least one nano-electro-  
3 mechanical system comprises:
- 4 a) at least one pattern of molecules wherein said at least one pattern of  
5 molecules is fabricated onto said nano-electro-mechanical system; and  
6 b) at least one molecular support genetically engineered into said portion of at  
7 least one chemical enzyme wherein said at least one molecular support is  
8 capable of binding to said at least one pattern of molecules.
- 1 22. The nanoscale engineered system of claim 21 wherein said at least one chemical  
2 enzyme is an ATP synthase complex.
- 1 23. The nanoscale engineered system of claim 21 wherein said at least one molecular  
2 support comprises an affinity tag.
- 1 24. The nanoscale engineered system of claim 21 wherein said molecular support  
2 comprises a histidine tag.
- 1 25. The nanoscale engineered system of claim 21 wherein said at least one pattern of  
2 molecules comprises a metal.
- 1 26. The nanoscale engineered system of claim 25 wherein said at least one pattern of  
2 molecules is selected from the group consisting of:  
3 a) copper;  
4 b) nickel;  
5 c) iron; and  
6 d) gold.

- 1 27. The nanoscale engineered system of claim 21 wherein said at least one pattern of  
2 molecules is comprised of a polymer.
- 1 28. The nanoscale engineered system of claim 21 wherein said at least one pattern of  
2 molecules is comprised of a composite with a binding affinity for an enzymatic  
3 tag.
- 1 29. The nanoscale engineered system of claim 19 wherein said nanoscale engineered  
2 system is a fluid pump.
- 1 30. The nanoscale engineered system of claim 19 wherein said nanoscale engineered  
2 system is a valve in a microfluidic device.
- 1 31. The nanoscale engineered system of claim 19 wherein said nanoscale engineered  
2 system is a source of motive power for a macroscopic medical device.
- 1 32. The nanoscale engineered system of claim 19 wherein said nanoscale engineered  
2 system is an electrical power source for a macroscopic medical device.
- 1 33. The nanoscale engineered system of claim 19 wherein said nanoscale engineered  
2 system is a chemo-mechanical power source for a macroscopic medical device.
- 1 34. The nanoscale engineered system of claim 19 wherein said nanoscale engineered  
2 system recognizes at least one cell type within an organism.
- 1 35. The nanoscale engineered system of claim 19 wherein said nanoscale engineered  
2 system recognizes at least one chemical agent within an organism.
- 1 36. The nanoscale engineered system of claim 19 wherein said nanoscale engineered  
2 system recognizes at least one environmental agent within an organism.
- 1 37. The nanoscale engineered system of claim 19 further comprising:  
2 a) at least one liposome comprising:  
3 i) at least one ATP synthase complex;

- 4                   ii) at least one bacteriorhodopsin protein wherein said at least one ATP  
5                   synthase complex and said at least one bacteriorhodopsin protein  
6                   are incorporated into a membrane of said liposome; and
- 7                   iii) a plurality of synthetic photosynthetic molecules;
- 8           b) a light source; and
- 9           c) a plurality of ATP molecules generated by a proton gradient produced in said  
10           membrane of said liposome wherein said nanoscale engineered system  
11           utilizes said plurality of ATP molecules to fuel said nanoscale engineered  
12           system.
- 1   38. The nanoscale engineered system of claim 37 wherein said nanoscale engineered  
2           system is autonomous.
- 1   39. The nanoscale engineered system of claim 20 wherein said portion of at least one  
2           ATP synthase complex is engineered to include at least one affinity binding site  
3           such that mechanical motion can be started and stopped depending upon whether  
4           said at least one affinity binding site is occupied wherein an occupation of said at  
5           least one affinity binding site prevents a conformational change necessary for  
6           ATP hydrolysis.
- 1   40. The nanoscale engineered system of claim 39 wherein said at least one affinity  
2           binding site is a metal binding site.
- 1   41. The nanoscale engineered system of claim 40 wherein said at least one metal binding  
2           site is a zinc-binding pocket.
- 1   42. The nanoscale engineered system of claim 41 wherein a plurality of zinc molecules  
2           can be added to said nanoscale engineered system such that said plurality of zinc  
3           molecules occupy said zinc-binding pocket and said portion of at least one ATP  
4           synthase complex stops mechanical motion.

1 43. The nanoscale engineered system of claim 42 wherein an EDTA compound can be  
2 added to said nanoscale engineered system such that said plurality of zinc  
3 molecules are removed from said zinc-binding pocket by said EDTA compound  
4 and said portion of at least one ATP synthase complex starts mechanical motion.

1 44. An expression vector comprising a portion of at least one ATP synthase complex  
2 expressed in said expression vector in a form such that said portion of at least one  
3 ATP synthase complex can be attached to at least one nano-electro-mechanical  
4 system.

1 45. A method of providing motive force to a nanoscale engineered system comprising:  
2 a) providing a portion of at least one ATP synthase complex that undergoes a  
3 conformational shift;  
4 b) coupling said portion of at least one ATP synthase complex to at least one  
5 nano-electro-mechanical system;  
6 c) generating ATP molecules with said portion of at least one ATP synthase  
7 complex; and  
8 d) utilizing a  $F_1$  subunit of said portion of at least one ATP synthase complex to  
9 catalyze ATP and generate energy for said nanoscale engineered system.

1 46. The method of claim 45 wherein said nanoscale engineered system is a fluid pump.

1 47. The method of claim 45 wherein said nanoscale engineered system is a valve in a  
2 microfluidic device.

1 48. The method of claim 45 wherein said nanoscale engineered system is an electrical  
2 power source for a macroscopic medical device.

1 49. The method of claim 45 wherein said nanoscale engineered system is a chemo-  
2 mechanical power source for a macroscopic medical device.

- 1 50. The method of claim 45 wherein said nanoscale engineered system recognizes at least  
2 one cell type within an organism.
- 1 51. The method of claim 45 wherein said nanoscale engineered system recognizes at least  
2 one chemical agent within an organism.
- 1 52. The method of claim 45 wherein said nanoscale engineered system recognizes at least  
2 one environmental agent within an organism.
- 1 53. A method of providing fuel for a nanoscale engineered system comprising:  
2 a) engineering at least one liposome such that said at least one liposome comprises:  
3 i) a portion of at least one ATP synthase complex;  
4 ii) at least one bacteriorhodopsin protein wherein said portion of at least one  
5 ATP synthase complex and said at least one bacteriorhodopsin  
6 protein are incorporated into a membrane of said liposome; and  
7 iii) a plurality of synthetic photosynthetic molecules;  
8 b) providing a light source;  
9 c) synthesizing a plurality of ATP molecules by utilizing said at least one  
10 bacteriorhodopsin protein and said light source to translocate a plurality of  
11 protons across said membrane such that a proton gradient is created and said  
12 portion of at least one ATP synthase complex produces said plurality of  
13 ATP molecules; and  
14 d) providing said plurality of ATP molecules as an energy source to power said  
15 portion of at least one ATP synthase complex coupled to said at least one  
16 nano-electro-mechanical system wherein said nanoscale engineered system  
17 harnesses a mechanical motion of said portion of at least one ATP synthase  
18 complex for motive power.

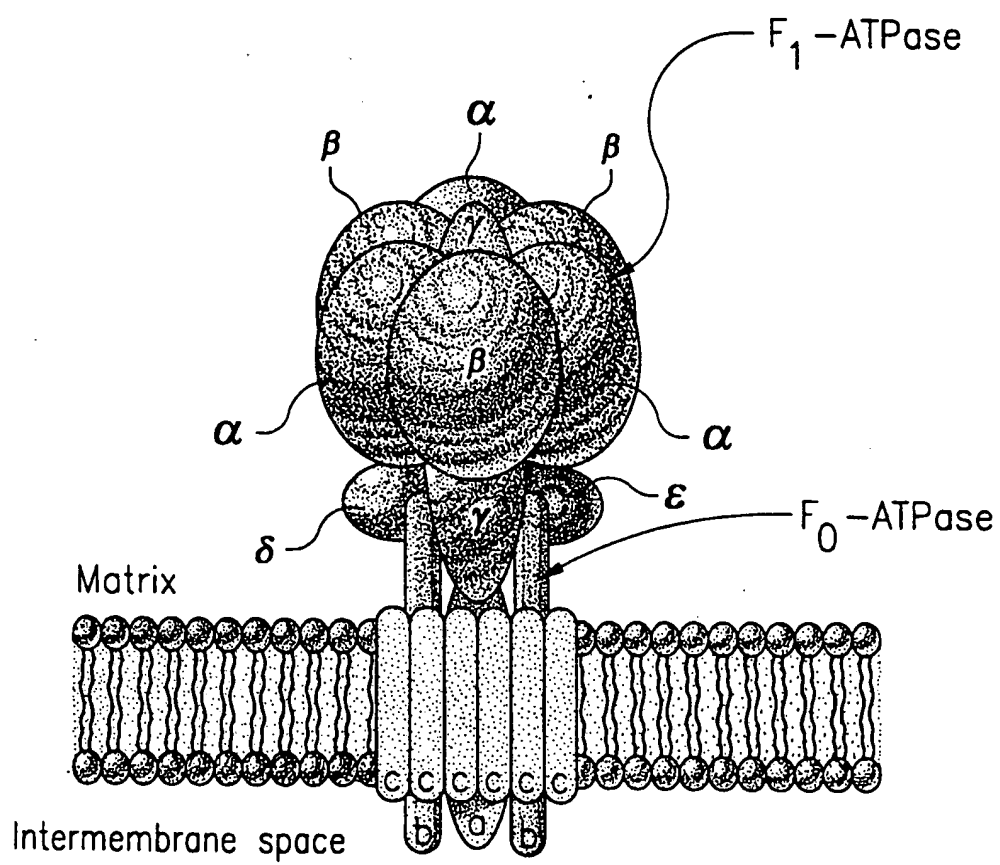
- 1 54. The method of claim 53 wherein said nanoscale engineered system is used to pump  
2 fluids.
- 1 55. The method of claim 53 wherein said nanoscale engineered system is used to open and  
2 close at least one valve in a microfluidic device.
- 1 56. The method of claim 53 wherein said nanoscale engineered system is used to provide a  
2 source of motive power for a macroscopic medical device.
- 1 57. The method of claim 53 wherein said nanoscale engineered system is an electrical  
2 power source for a macroscopic medical device.
- 1 58. The method of claim 53 wherein said nanoscale engineered system is a chemo-  
2 mechanical power source for a macroscopic medical device.
- 1 59. The method of claim 53 wherein said nanoscale engineered system recognizes at least  
2 one cell type within an organism.
- 1 60. The method of claim 53 wherein said nanoscale engineered system recognizes at least  
2 one chemical agent within an organism.
- 1 61. The nanoscale engineered system of claim 53 wherein said nanoscale engineered  
2 system recognizes at least one environmental agent within an organism.
- 1 62. A method of controlling a nanoscale engineered system comprising:  
2 a) modifying a portion of at least one ATP synthase complex to include at least one  
3 affinity binding site such that mechanical motion can be started and stopped  
4 depending upon whether said at least one affinity binding site is occupied  
5 wherein an occupation of said at least one affinity binding site prevents a  
6 conformational change necessary for ATP hydrolysis;  
7 b) coupling said portion of at least one ATP synthase complex to at least one nano-  
8 electro-mechanical system;

- 9           c) adding a plurality of molecules to said nanoscale engineered system such that  
10           said plurality of molecules occupy said at least one affinity binding site and  
11           said portion of at least one ATP synthase complex stops mechanical motion;
- 12           d) adding at least one compound to said nanoscale engineered system such that said  
13           at least one compound removes said plurality of molecules from said at least  
14           one affinity binding site, and said portion of at least one ATP synthase  
15           complex starts mechanical motion; and
- 16           e) repeating steps c) and d) as necessary such that said portion of at least one ATP  
17           synthase complex stops or starts mechanical motion.
- 1   63. The method of claim 62 wherein said at least one affinity binding site is a metal  
2       binding site.
- 1   64. The method of claim 63 wherein said at least one metal binding site is a zinc-binding  
2       pocket.
- 1   65. The method of claim 62 wherein said plurality of molecules is a plurality of zinc  
2       molecules.
- 1   66. The method of claim 62 wherein said at least one compound is an EDTA compound.
- 1   67. The method of claim 62 wherein said nanoscale engineered system is used to pump  
2       fluids.
- 1   68. The method of claim 62 wherein said nanoscale engineered system is used to open and  
2       close at least one valve in a microfluidic device.
- 1   69. The method of claim 62 wherein said nanoscale engineered system is used to provide a  
2       source of motive power for a macroscopic medical device.
- 1   70. The method of claim 62 wherein said nanoscale engineered system is an electrical  
2       power source for a macroscopic medical device.

- 1 71. The method of claim 62 wherein said nanoscale engineered system is a chemo-  
2 mechanical power source for a macroscopic medical device.
- 1 72. The method of claim 62 wherein said nanoscale engineered system recognizes at least  
2 one cell type within an organism.
- 1 73. The method of claim 62 wherein said nanoscale engineered system recognizes at least  
2 one chemical agent within an organism.
- 1 74. The method of claim 62 wherein said nanoscale engineered system recognizes at least  
2 one environmental agent within an organism.
- 1 75. A method of detecting a molecular rotation of a molecular motor comprising:
- 2 a) attaching a molecular tag that is readily visible under an optical microscope to a  
3 structural element of said molecular motor; and
- 4 b) monitoring said molecular tag to observe said molecular rotation of said  
5 molecular motor.
- 1 76. The method of claim 75 wherein said molecular tag is a fluorescently labeled  
2 biotinylated actin filament.
- 1 77. The method of claim 75 wherein said structural element of said molecular motor is a  $\gamma$   
2 subunit of a portion of at least one ATP synthase complex.

1/9

FIG. 1



2/9

FIG. 2

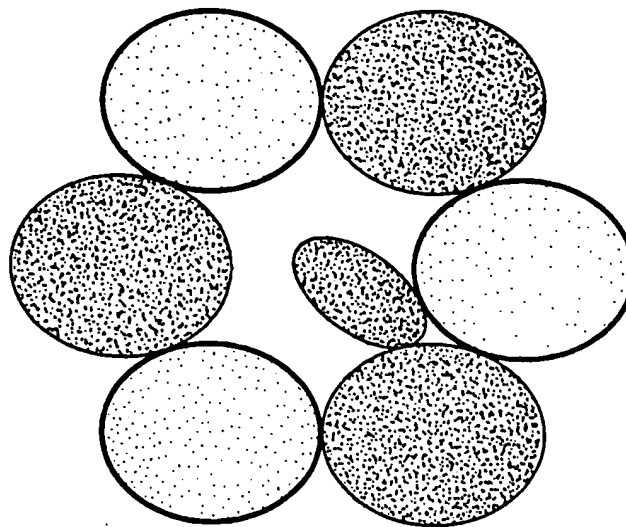
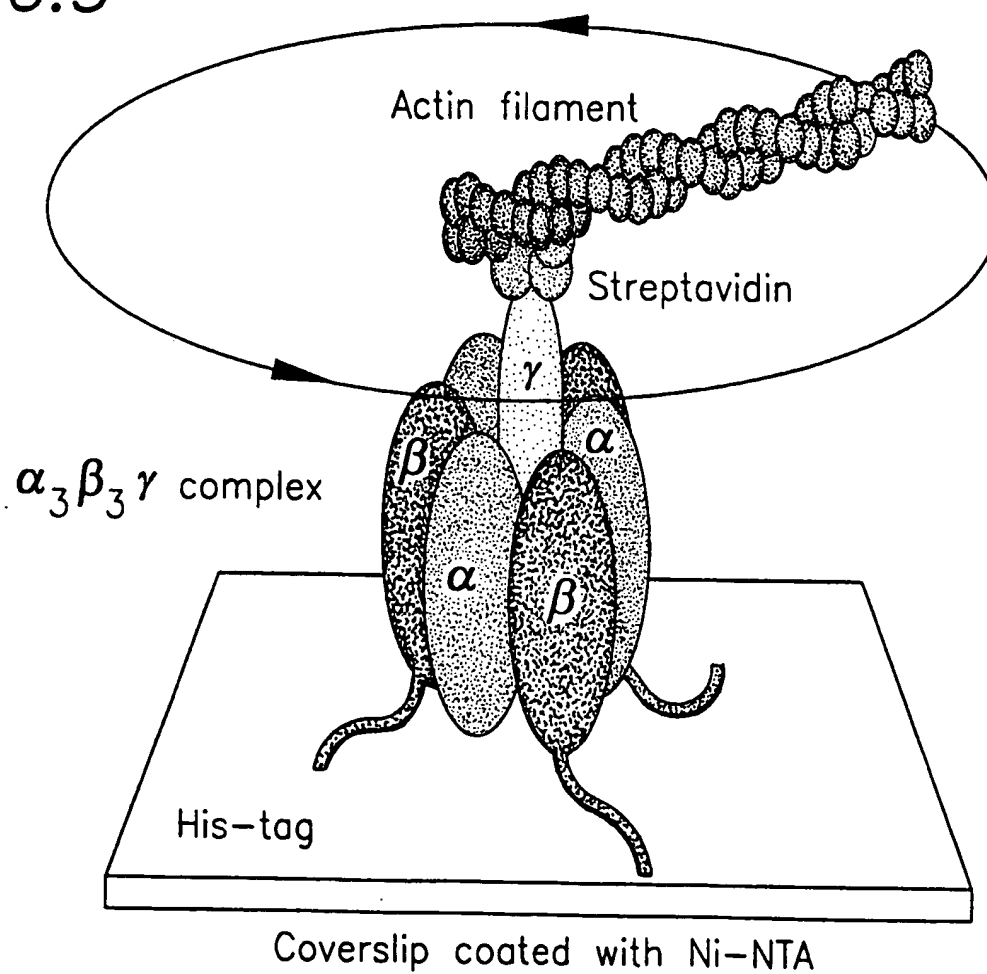


FIG. 3



3/9

FIG. 4

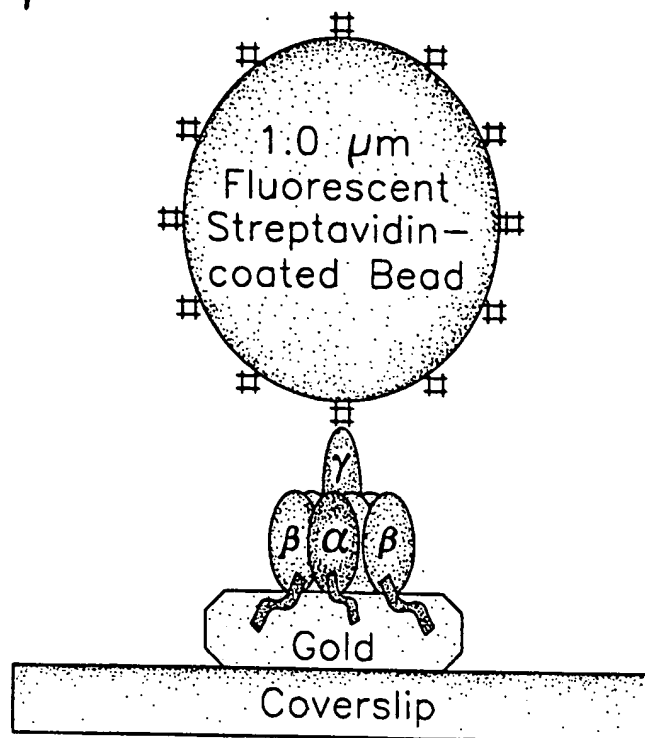
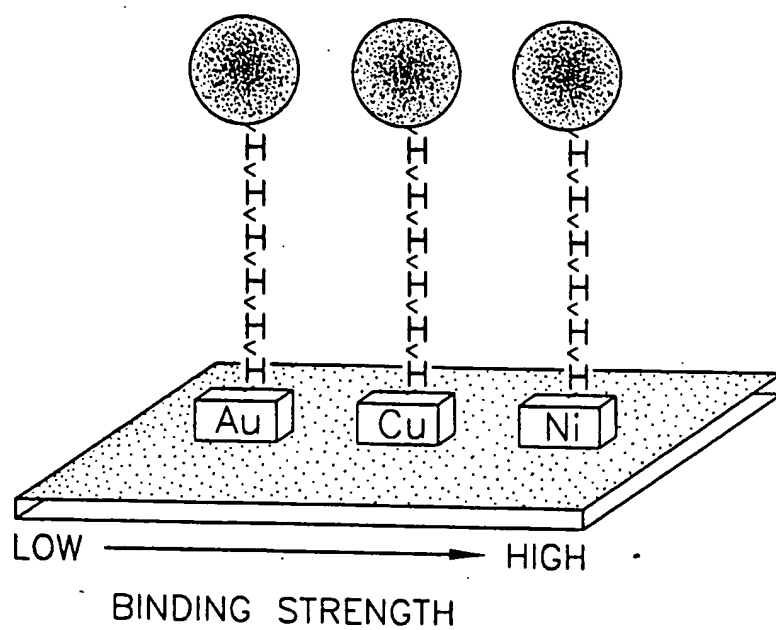
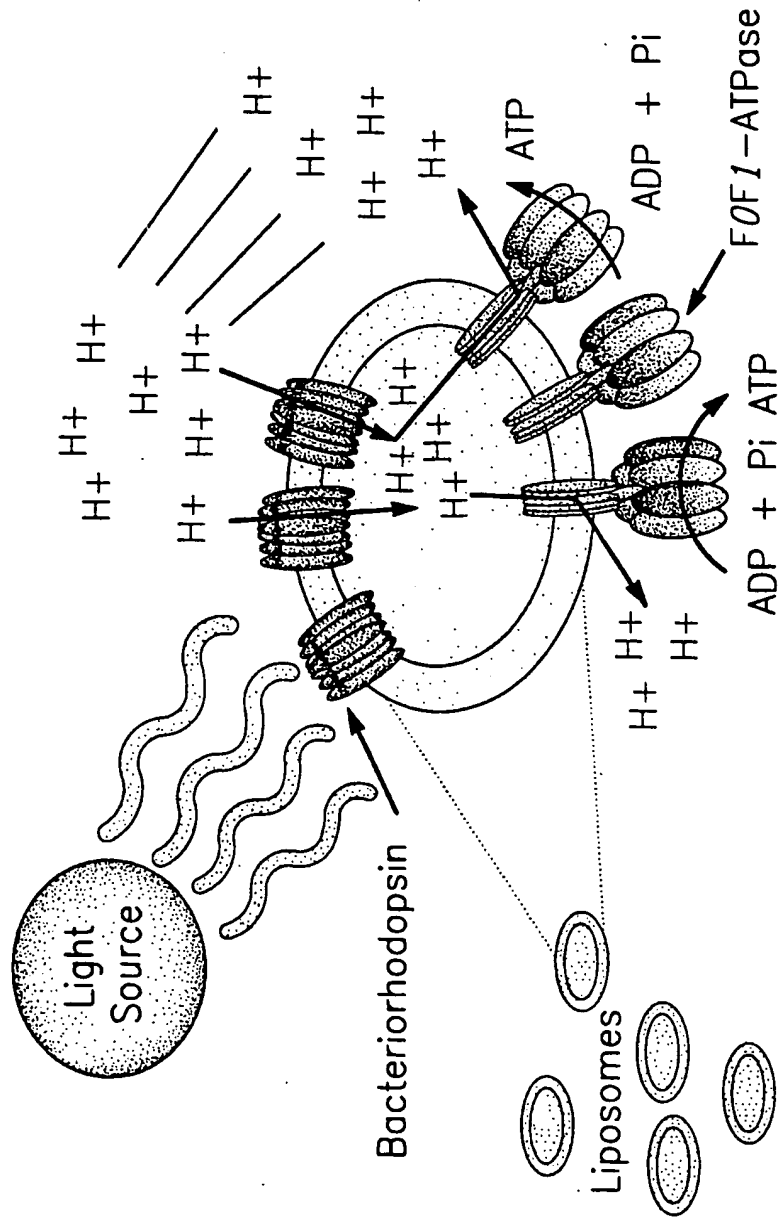


FIG. 5



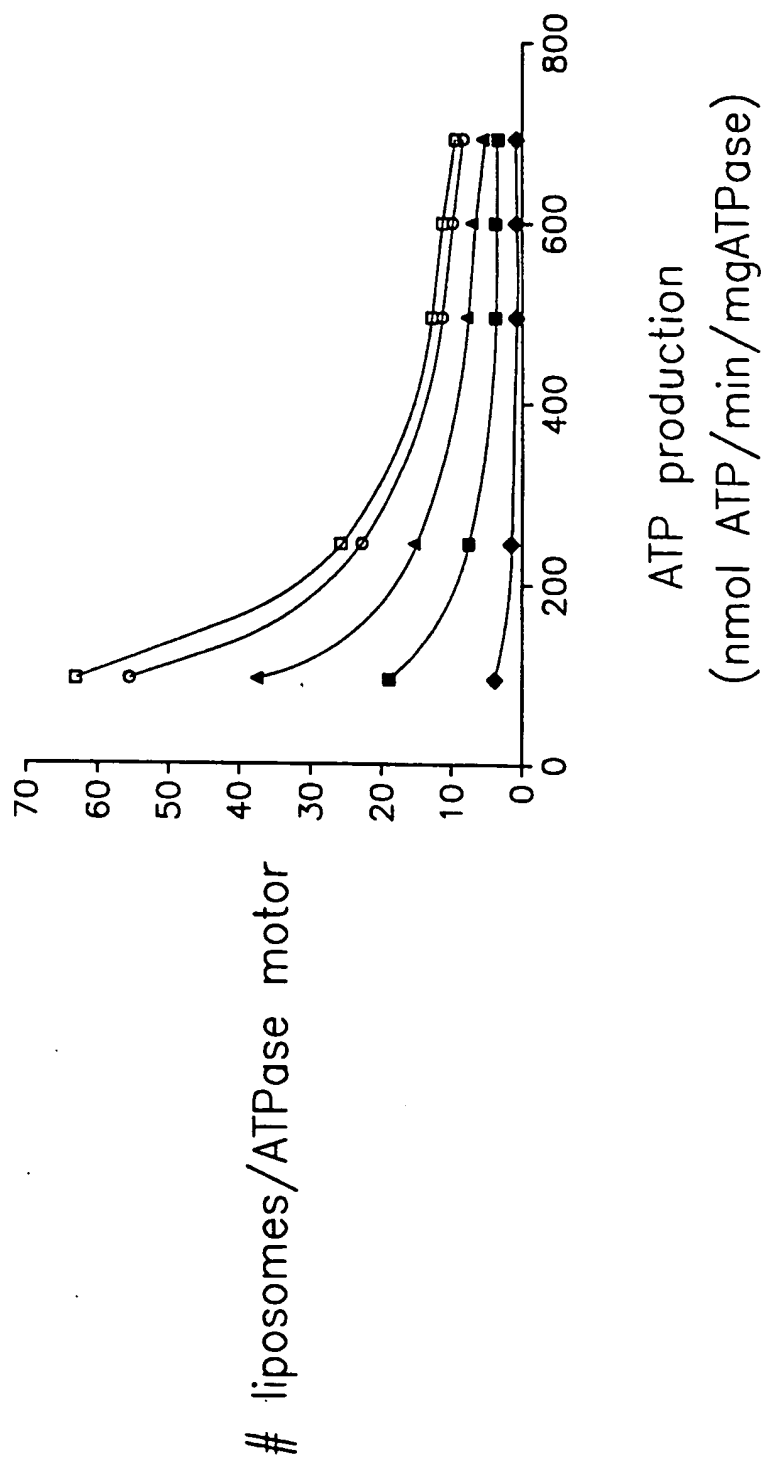
4/9

FIG. 6



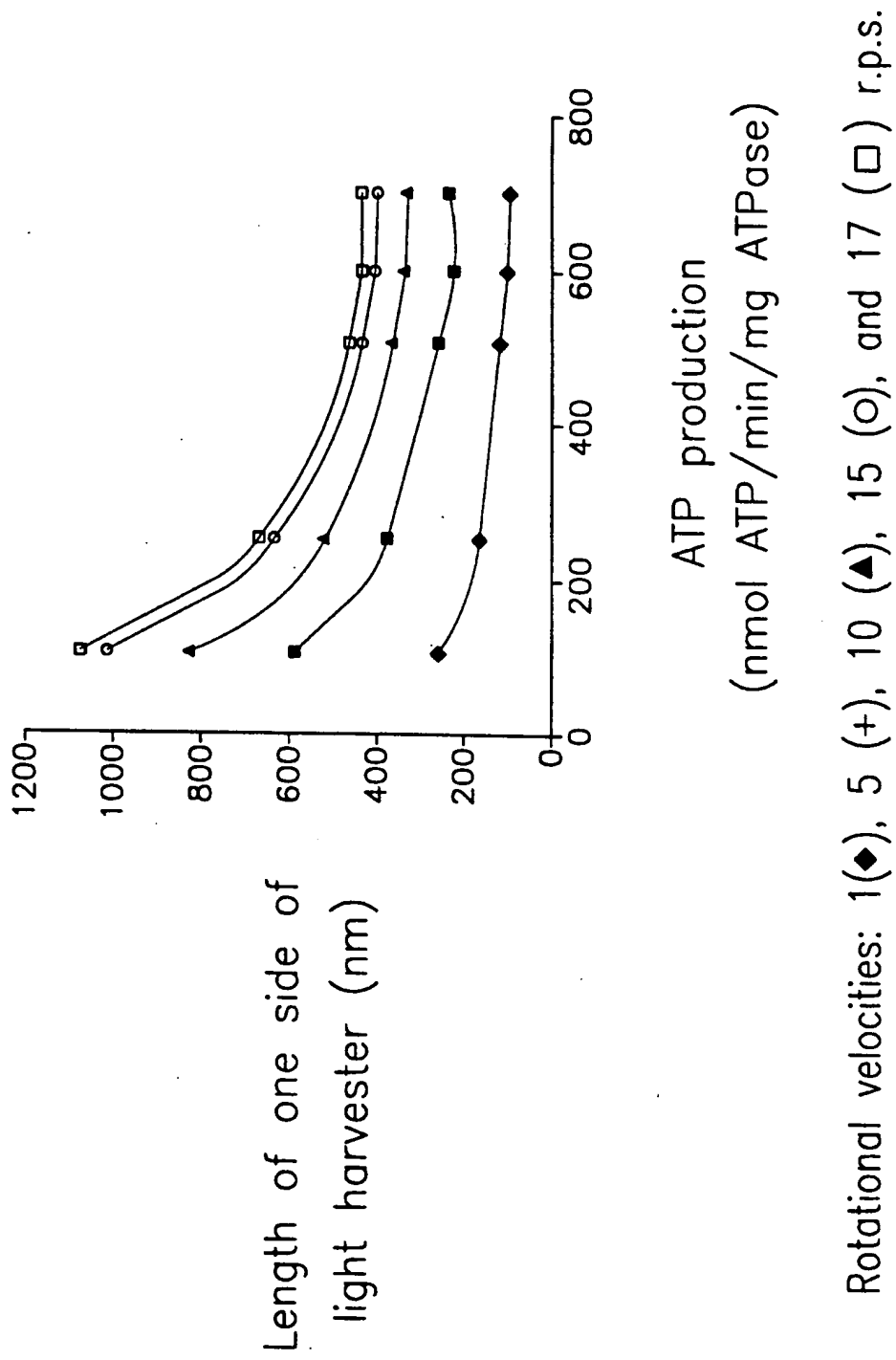
5/9

FIG. 7



6/9

FIG. 8



7/9

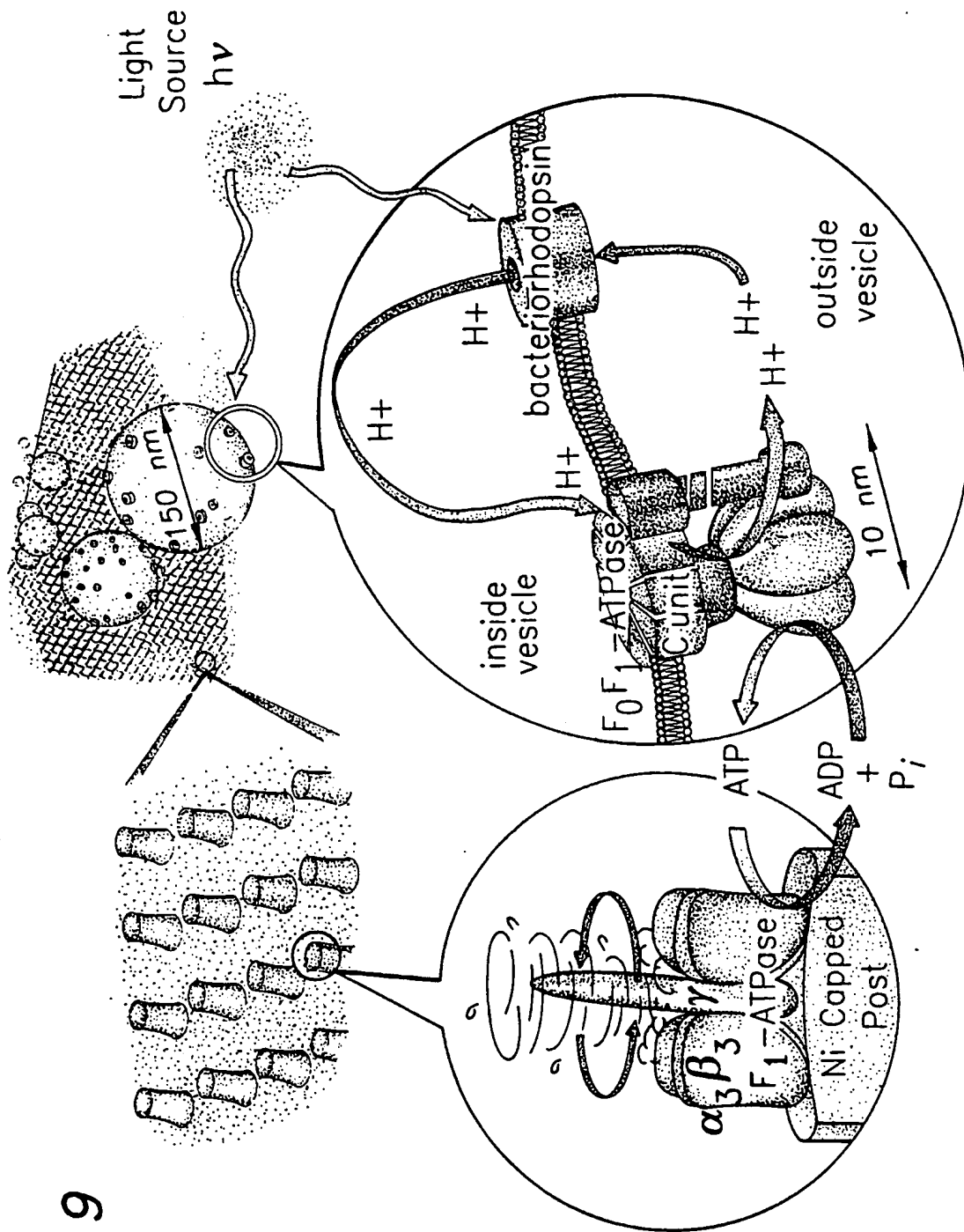
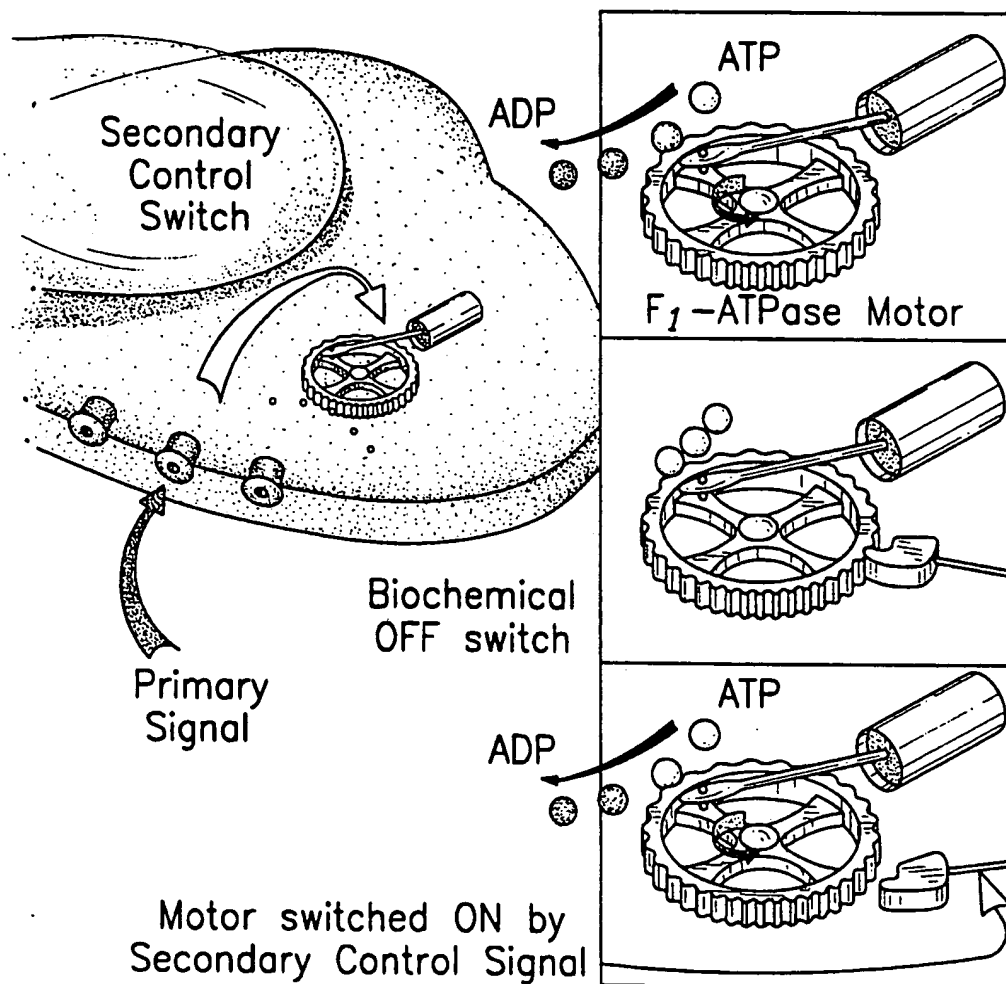


FIG. 9

8/9

FIG. 10



9/9

FIG. 11

